Int J of Soc Robotics (2015) 7:371–392
DOI 10.1007/s12369-014-0276-5

A Neural Architecture for Performing Actual and Mentally Simulated Movements During Self-Intended and Observed Bimanual Arm Reaching Movements

Rodolphe J. Gentili · Hyuk Oh · Di-Wei Huang · Garrett E. Katz · Ross H. Miller · James A. Reggia

Accepted: 12 December 2014 / Published online: 14 January 2015

Abstract Dexterous reaching, pointing, and grasping play a critical role in human interactions with tools and the environment, and it also allows individuals to interact with one another effectively in social settings. Developing robotic systems with mental simulation and imitation learning abilities for such tasks seems a promising way to enhance robot performance as well as to enable interactions with humans in a social context. In spite of important advances in artificial intelligence and smart robotics, current robotic systems lack the flexibility and adaptability that humans so naturally exhibit. Here we present and study a neural architecture that captures some critical visuo-spatial transformations that are required for the cognitive processes of mental simulation and imitation. The results show that our neural model can perform accurate, flexible and robust 3D unimanual and bimanual actual/imagined reaching movements while avoiding extreme joint positions and generating kinematics similar to those observed with humans. In addition, using visuo-spatial transformations, the neural model was able to observe/imitate bimanual arm reaching movements independently of the viewpoint, distance and anthropometry between the demonstrator and imitator. Our model is a first step towards developing a more advanced neurally-inspired hierarchical architecture that integrates mental simulation and sensorimotor processing as it learns to imitate dexterous bimanual arm movements.

Keywords Mental simulation · Movement imitation · Bimanual reaching movements · Motor learning · Internal models · Inverse kinematics · Neural network models

Electronic supplementary material The online version of this article (doi:10.1007/s12369-014-0276-5) contains supplementary material, which is available to authorized users.

R. J. Gentili (✉) · R. H. Miller
Department of Kinesiology, School of Public Health, University of Maryland, College Park, MD 20742, USA
e-mail: rodolphe@umd.edu

H. Oh
Neuroscience and Cognitive Science Program, University of Maryland, College Park, MD 20742, USA

D.-W. Huang · G. E. Katz · J. A. Reggia
Department of Computer Science, University of Maryland, College Park, MD 20742, USA

1 Introduction

The ability to point, reach and grasp objects is a fundamental element of the human motor repertoire [1,2]. This is true not only because it allows people to interact with their environment, but also because it allows people to interact with one another effectively in social settings. This has become progressively more important during recent years as robots increasingly interact with humans in the workplace, in rehabilitation settings and even in the home. For example, one critical issue in such human–robotic social interactions is how we can produce robots that can mentally simulate their actions to predict appropriate responses with respect to the environment in the presence of humans and also to learn easily via imitation, i.e., "programming by demonstration" [3–12]. Developing robots with such mental simulation and imitation learning capabilities could (i) qualitatively reduce the problem of programming robots to perform specific tasks, (ii) broaden the range of people who could train robots and (iii) provide more life-like humanoid robots that enhance human–robot interactions in a social context and in turn inform human performance.

However, developing robots capable of mentally simulating and learning actions such as reaching and grasping in social settings has proven to be a very challenging task. The

flexibility of human upper limbs allows for reaching different spatial locations by producing various trajectories and paths, thus providing not only a high flexibility in daily activities but also a high level of ambiguity during imitation learning. An important key ingredient of such arm versatility and kinematic redundancy is that it allows the hands to reach the same targets with various postures while staying away from the joint limits (i.e., to reach more comfortable postures) as well as avoiding objects/obstacles and limb interferences [1]. From a motor control and learning standpoint, such kinematic redundancy complicates the problem of controlling the arm since it is relatively difficult to generate an appropriate movement plan for dexterous reaching performance with so many potential solutions available. This is due to the fact that the transformation between sensory and motor spaces is highly nonlinear and depends on the constraints imposed by the physical characteristics of the human arms. It is also due to an environment that constantly changes and involves the presence of multiple obstacles, perturbations and constraints that imply sudden movement redirection within the workspace. Despite such complexity, many past studies focusing on human arm movements have revealed that Cartesian and joint kinematics are highly stereotyped, indicating robust invariant spatio-temporal features such as sigmoid displacements as well as single-peaked and bell-shaped velocity profiles [13–18]. As such, the performance of redundant, multi-jointed upper limbs depends on accurate, robust and flexible movement planning and learning capabilities when performing bimanual arm reaching movements in 3D.

In addition to such upper-extremity versatility, a critical component in producing such superior performance for dexterous manipulations is the human ability to mentally plan as well as simulate and predict the consequences of one's own actions through covert cognitive-motor processes. By mental simulation we mean the covert re-enactment of cognitive-motor and sensorimotor states acquired during previous interactions with the environment. This enables a person to reach a goal, and to act anticipatorily and not just simply reactively. In particular, the motor neuroscience literature suggests that capabilities such as the ability to: (i) mentally simulate and predict the sensory consequences of our own movements, (ii) mentally manipulate objects/environments (e.g., mental rotation of objects, workspace) and (iii) recognize, imitate and predict others' actions, are all critical to performing and interacting efficiently in a changing environment at the sensorimotor as well social level [1,18–20].

Based on experimental works in humans, a *mental simulation theory* was proposed and suggests that the motor system is included within a simulation network that, when activated, allows the performance of both actual and mental (or imagined) self-intended movements as well as the observation and imitation of movements executed by other individuals [21].

Here these four modalities of movement performance are defined as: (i) self-intended actual movements are overtly carried-out by the individual; (ii) self-intended mental movements are covertly performed by the individual without any overt motor output; (iii) observed movements that are physically executed by another individual (i.e., a demonstrator) which engage the observer in mental simulation of the same movements (no overt motor output) and iv) imitated movements performed by an individual (i.e., an imitator) that were previously and overtly executed by another individual (i.e., a demonstrator).This mental simulation theory has been supported by many studies which have shown that humans exhibit similar behaviors and activation of cortical and subcortical brain structures during actual (i.e., overtly executed) and mental (i.e., covertly executed or imagined) actions [21–27]. It was also suggested that this simulation network incorporates a fronto-parietal network that is an important component of the human mirror neuron system (MNS) during movement observation [28–32]. Therefore, mental simulation theory provides a unified framework for mechanisms that can execute actual and mental self-intended actions as well as observed and imitated actions performed by another individual [21].

Despite important advances in the field of artificial intelligence and smart robotics, current robotic systems lack the flexibility, dexterity and adaptability that humans so naturally exhibit when performing motor actions such as unimanual/bimanual reaching and grasping. As such, it appears reasonable to consider that the embodiment of similar cognitive-motor processes in robotic control systems could enhance them by providing a more human-like dexterity, flexibility, adaptability and robustness [33–37]. This is particularly important since there has recently been a rapid increase of robots' computing capabilities that have enhanced the humanoid mechanical capabilities of their upper extremities (e.g., Shadow, DLR, and Baxter robotic systems).

Specifically, although the notions of hierarchical control [9], mental simulation [12] and learning by imitation [5] were considered, albeit generally independently of each other, in previous computational work, there is still a critical need to develop a unified neurally-inspired multilevel architecture that coherently integrates (i) a high cognitive level (e.g., role of the human prefrontal cortex (PFC) in abstract planning to define an action sequence) with (ii) a low sensorimotor level (e.g., role of the human premotor, primary motor and parietal cortices in trajectory planning, sensorimotor predictions and execution) in order to perform both self-intended actual/mental as well as imitated/observed reaching and grasping actions. Therefore, our long-term goal is to develop a neurally inspired hierarchical architecture that includes a multi-level simulation network for coherently integrating high (cognitive) and low (sensorimotor) levels.

Here we take some first steps in developing such a comprehensive model. The neural architecture that we describe in this paper captures some critical visuo-spatial transformations that are needed for the cognitive processes of mental simulation and imitation. Specifically, our neural architecture includes important components of the fronto-parietal brain circuits, and is motivated by three primary considerations.

First, although interesting, most previous work related to unimanual/bimanual arm coordination and movement imitation in humanoid robots has generally employed robotic techniques (e.g., impedance control, extended Jacobian method, statistical methods) with little biological relevance such as explicit inversion or optimization procedures to implement inverse kinematics computation of the arms [38–46]. Conversely, building upon the knowledge of human motor neuroscience, another approach has been to propose biologically inspired neural models (with various degrees of biological plausibility) to develop robotic control systems [5,9–12,47–57]. The presented work is in line with this latter approach in proposing a neurally inspired control system for bilateral reaching movements.

Second, consistent with the bio-inspired approach, previous neural models developed for imitation learning generally do not include a neural component that can learn to compute the visuo-spatial transformation of the frame of reference between a demonstrator and an imitator [48–52,58–63]. This is critical since it allows one to implement (and link to other sensorimotor systems) a mechanism that allows for imitating an action independently of the differences in viewpoint, distance and anthropometry between a demonstrator and an imitator [63–66].

Third, on the one hand, past neurally inspired models proposed for imitation learning in robotics do not generally account for mental simulations whereas, on the other hand, previous models using mental simulation for robotic systems do not include imitation and were mainly developed for navigation but not for bilateral arm reaching and grasping [5,10–12,48–53,67–70].

As such, at this developmental stage our neurally-inspired architecture can be distinguished by its inclusion of neural modules that are able to: (i) compute arm inverse kinematics through sensorimotor learning by exploration of self-intended movements in order to generate accurate and flexible trajectories; (ii) deal with changing environmental conditions (e.g., various types of perturbations) during actual arm reaching movements; (iii) perform a frame of reference transformation from allo- to ego-centric coordinates by executing multiple visuo-spatial transformations during learning, including the rotation and translation of the workspace as well as size rescaling (personalization) of an observed individual demonstrator and (iv) imitate coordinated unimanual and bimanual multidirectional arm movements observed from a demonstrator having a different limb configuration and different anthropometry, and observed from different points of view and distances during multiple types of tasks (e.g., mirror symmetric and asymmetric movements).

2 Materials and Methods

In this section we first describe the overall architecture formed by three fronto-parietal cortical circuits in our neural architecture (Sect. 2.1). Then, the most critical components and their detailed implementation are presented in Sects. 2.2 and 2.3, respectively. Section 2.4 presents how the performance of the neural architecture was assessed.

2.1 Computational and Physiological Characteristics of the Neural Architecture

From a computational point of view, in order to provide the neural architecture with the capabilities to actually execute and mentally simulate self-intended movements, as well to observe and imitate actions executed by another individual, three main neural circuits need to be considered (Fig. 1).

A first circuit allows actual execution of arm movements that include the sensorimotor transformation between the goal and the neural command (inverse model) that is sent to the arms. Such sensorimotor transformation is implemented by a neural network that functionally mimics the motor/premotor cortices where the goal of the movement is received from the prefrontal regions in order to compute the neural command sent to the arms [54–56]. In turn, the actual consequence of this motor command conveyed by the peripheral feedback (from actual motion) that can be used to modify the neural drive if needed. The movement computed by this circuit which is triggered by signals (likely generated by the basal ganglia [71] or the PFC [72]) that release the neural drive sent to the periphery to move the limbs.

A second fronto-parietal circuit allows for mental simulation of sensorimotor consequences of arm movements. In this case, the trigger signals for the actual movement is intercepted through an inhibitory mechanism (gating system, see method Sect. 2.2.2) and thus no overt motor output exists. Computationally, this second circuit includes the same inverse sensorimotor transformation implemented in the motor/premotor regions (inverse model). Although the actual motor command is blocked, a copy of efference of this neural drive is still available to a predictive system (forward model) located in the posterior parietal cortex (PPC) and in particular the intraparietal lobule (IPL). This copy allows prediction of the corresponding sensorimotor consequences [73,74]. These predictions are then sent back to the motor/premotor regions (inverse model) to guide the computation of the neural command. As such this forms an internal simulation loop that can also be recruited using a trigger sig-

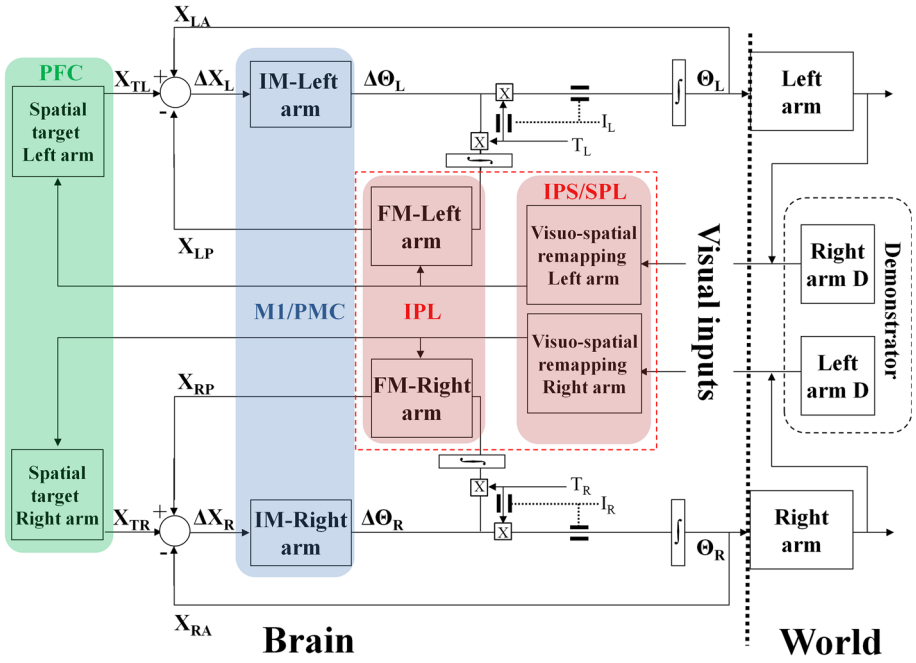

Fig. 1 Overview of the structure of the neural architecture for unimanual and bimanual arm movements. The inverse model (IM) and the visuo-spatial remapping are implemented using neural networks. The forward model (FM) is implemented using a closed form function. X and Θ represent the spatial and joint position. XT{R,L}, X{R,L}A,P represent the target, actual and predicted spatial position for the *right* (R) or *left* (L) arm. ΔX{R,P}: spatial displacements for the *right* (R) or *left* (L) arm. T{R,L} indicate the trigger signals for the for the *right* (R) or *left* (L) arm that multiplies the output of the IM (see small *square* including a cross). I{R,L} indicate the inhibitory signals for the for the *right* (R) or *left* (L) arm that close or open the gates represented as two small parallel *thick lines*. The *green*, *blue* and *red* areas represent the prefrontal, motor/premotor and parietal regions, respectively. (Color figure online)

nal. It was suggested that such computational mechanisms are used in humans during mental simulation of motor performance, and thus explaining why similar movement duration and activation of cortical regions, cerebellum and basal ganglia were observed for both overt and covert reaching movements [18,19,22,75]. Since these two circuits are involved in the computation of the neural drive and sensorimotor prediction, we consider them as the low level system of the model.

A third fronto-parietal circuit remaps an observed movement from the demonstrator's to the imitator's frame of reference. Computationally, this circuit includes neural networks that receive as inputs the visual inputs of the observed movement in allocentric coordinates and transform those visual inputs into the corresponding egocentric coordinates. Such a neural network would correspond to the intraparietal sulcus and superior parietal lobule (IPS/SPL) since those brain regions were evidenced as critical for humans to perform frame of reference scaling and viewpoint transformations [76–79]. These remapped visual inputs are then sent to the two circuits mentioned above (including an inverse and forward model) allowing thus for mental simulation and observation/imitation of observed movements [78,79]. Such allo- to ego- centric coordinate transformation is performed independently of the viewpoint and distance between the imitator and the demonstrator as well as the demonstrator's anthropometry [78,79]. This last circuit implementing these visuo-spatial transformations is also considered to be a low level system, although its nature tends to be slightly more cognitive.

Thus, overall the proposed fronto-parietal architecture is, at least in part, consistent with the simulation network (mental simulation theory) that is recruited to perform self-intended actual and mental [21,80,81], observed/imitated movements (frontal/parietal MNS) as well as mental rotation [28–32,76,77,79].

At this developmental stage of our neural architecture, it focuses on kinematics without including the dynamics of effectors and objects since it aims to place the arms in the neighborhood of an object (e.g., box) or part of the object (e.g., top or lateral handle of the box) independently of information about the object's properties such as surface texture and position of the fingers on the object. Also, in this early version, the model does not learn to imitate arm movements directly using imitation learning but rather learns by employing a combination of self-intended actual movement during an exploratory phase as well as by performing visuo-spatial transformations such as mental rotation and personalization.

The controllers for the right and left arms are based on the same structure using the same computational circuits. They control independently the two arms to allow both unimanual and bimanual arm control (Fig. 1).

2.2 Cortical Model for Neural Drive Generation and Sensorimotor Predictions

2.2.1 *Cortical Model for Computation of the Neural Commands and Prediction of Sensorimotor Consequences*

The neural architecture presented here directly extends a previous cortical model of reaching [54,55] that functionally reproduces the population vector coding processes observed in the motor/premotor regions [82]. It must be noted that such a model does not explicitly capture the anatomical cortical circuitry. Rather this neural architecture employs an internal model of the forward and inverse kinematic mappings in order to accurately control an anthropomorphic robot arm with seven DOFs in 3D while keeping comfortable joint configurations of the effector [55]. In other words, this neural model encodes the mapping between the displacements of the joints and of the arm by encoding the joint-to-spatial (forward kinematic model) and the spatial-to-joint (inverse kinematic model) transformations. This neural controller can adaptively perform upper limb movements in 3D due to the encoding of these kinematics in internal models that are learned by integrating five multiple types of sensorimotor information. The first type is visual information related to the localization of the arm and of the targets in the 3D workspace. The second was the proprioceptive information that encodes the current state of the arm (e.g., joint positions) resulting from the sensory consequences of the motor commands that were available either from internal predictions generated by the forward model or from peripheral feedback. Other sensorimotor information includes the neural drive that conveys information to control the upper limb, the task and the goal-related information involved in motor planning as well as the motor error (e.g., computed by the cerebellum; [57,83]). This multiple-type sensorimotor information is combined in order to tune the neural model parameters during learning of the inverse model to generate the appropriate motor commands that produce the joint displacements. In addition, the system learns to maintain the joint angles close to their natural range and thus, as much as possible, to comfortable arm postures [55].

2.2.2 *Architecture, Learning and Performance of the Sensorimotor Cortical Networks*

The relationship between spatial and joint velocities of the anthropomorphic arm can be expressed according to the following equation:

$$\Delta X = J(\theta)\Delta\Theta \tag{1}$$

where $\Delta X = [\Delta x\ \Delta y\ \Delta z]$, $\Delta\Theta = [\Delta\theta_1\ \Delta\theta_2\ \Delta\theta_3\ \Delta\theta_4\ \Delta\theta_5\ \Delta\theta_6\ \Delta\theta_7]$ and J are the spatial velocity, the joint velocity and the Jacobian matrix of the simulated robotic arm, respectively. The internal forward kinematic model of the arm was modeled using the closed-form kinematics model of the arms and takes as inputs the joints and provides as outputs the spatial coordinates. The inverse model was obtained according to the following approach based on [55]. To obtain a joint rotation vector that moves the arm at a desired spatial velocity, (1) can be rewritten as follow:

$$\Delta\Theta = G(\theta)\Delta X \tag{2}$$

where $G(\theta) = J^{-1}(\theta)$ is a pseudo-inverse of the Jacobian matrix.

In addition, among the multiple possible joint velocity that move the arm in the desired spatial velocity, it is possible to select those that will tend to move the joints through the middle of their ranges of motion as much as possible. This additional component refers to the notion of postural relaxation that can be implemented by employing a stationary vector $R(\theta)$ that tends to position the arm in a comfortable joint posture [55,84,85]. Thus (2) can be rewritten as:

$$\Delta\Theta = G(\theta)\Delta X + R(\theta) \tag{3}$$

where $R(\theta)$ is the postural relaxation vector.

The approximation of the elements of the matrix $G(\theta)$ is performed using a form of hyperplane radial basis function (HRBF) network [55,86,87]. Each element of $G(\theta)$ is denoted by $g_{ij}(\theta)$, where indices i and j refer to the joint space ($n = 7$) and the 3D workspace ($n = 3$) dimensions, respectively. $G(\theta)$ was implemented by employing a radial basis function network that changes its activity when recognizing a particular joint configuration (θ) as inputs [55]. The outputs of network $g_{ij}(\theta)$ and $r_i(\theta)$ are given by the following equations:

$$g_{ij}(\theta) = \sum_k \left(\frac{A_{ijk}}{\sum_k A_{ijk}}\right)\left(w_{ijk} + \sum_m c_{ijkm} z_{ijkm}\right) \tag{4}$$

$$c_{ijkm}(\theta) = \frac{\theta_m - \mu_{ijkm}}{\sigma_{ijkm}} \tag{5}$$

$$A_{ijk} = e^{-\sum_l c_{ijkl}^2} \tag{6}$$

$$r_i(\theta) = \sum_k \left(\frac{A_{ik}}{\sum_k A_{ik}}\right)\left(w_{ik} + \sum_m c_{ikm} z_{ikm}\right) \tag{7}$$

The following learning rules based on gradient descent were employed in order to update the parameters of the network $G(\theta)$:

$$\Delta w_{ijk} = -2\alpha_G \left(\Delta\Theta^{Ri} - \Delta\Theta^{i}\right)\left(\Delta X_j\right) h_{ijk} \tag{8}$$

$$\Delta z_{ijkm} = -2\alpha_G \left(\Delta\Theta^{Ri} - \Delta\Theta^{i}\right)\left(\Delta X_j\right) h_{ijk} c_{ijkm} \tag{9}$$

The following learning rules were employed in order to update the parameters of the network R(θ):

$$\Delta w_{ik} = -2\alpha_R \left(\Delta\Theta^{Ri} - \Delta\Theta^{i}\right) + \frac{\beta_i}{\theta_i^r}\left(\frac{\theta_i - \theta_i^c}{\theta_i^r}\right) h_{ik} \quad (10)$$

$$\Delta z_{ikm} = -2\alpha_R \left(\Delta\Theta^{Ri} - \Delta\Theta^{i}\right) + \frac{\beta_i}{\theta_i^r}\left(\frac{\theta_i - \theta_i^c}{\theta_i^r}\right) h_{ik} c_{ikm} \quad (11)$$

where k is the index of the basis function, the vector c_{ijkm} represents the distance between the input value θ and the center of the k^{th} basis function, α_G and α_R are the learning rates (empirically chosen) and A_{ijk} is the activation of the basis function with a Gaussian function where μ_{ijkm} and σ_{ijkm} are the centers and the standard deviations along the dimension m of the k^{th} Gaussian activation function ($n = 2, 187$), respectively. Each basis function is associated with a weight w_{ijk}, related to the amount of the data 'under its receptive field'. The set of weights z_{ijkm} allows for local and linear approximation of the slope of the data 'under its receptive field'. These neural weights were modified throughout learning by presenting random training data to the neural network during a babbling phase described next.

The learning strategy consisted of a random sensorimotor exploration cycle in which successive action–perception cycles are performed. As such the system produces motor commands to perform multiple arm movements towards random spatial targets to cover the entire 3D workspace. In particular, each action–perception cycle is implemented as follows. First random joints displacements ($\Delta\Theta^R$) are endogenously generated from the present joint configurations (Θ) that were sent as inputs to the neural model and also to the arm to perform the corresponding joint configuration. Concurrently, the forward model generates the corresponding spatial displacements (ΔX) of the hand in the 3D workspace that are then provided to the cortical architecture. Based on these spatial displacements, the cortical model estimates the corresponding joint displacements ($\Delta\hat{\Theta}$) and compares them to those randomly generated, providing thus an error signal to guide the adaptation of the network parameters (w_{ijk}, z_{ijkm} in (8)–(11)) [55,86]. A model of the kinematics chain of an actual human redundant arm including seven degrees of freedom (DOFs) was obtained by using the Denavit–Hartenberg parameterization to model the two upper limb effectors [88]. The glenohumeral shoulder joint was modeled with three revolute joints including rotation (θ_1), adduction-abduction (θ_2) and flexion-extension (θ_3), respectively. The elbow joint was modeled with two revolute joints [89] in order to permit movement of flexion-extension (θ_4) and pronation-supination (θ_5). The hand was connected to the arm through the wrist joint which controls the hand orientation in order to perform movements of adduction-abduction (θ_6) as well as flexion-extension (θ_7) (for further details, see Appendix 1—Supplementary material).

After learning, trigger signals (called '$T_{R/L}$' signals) were used to convert a motor plan into an overt (self-intended actual or imitated) or covert (self-intended imagined or observed) action, and this was combined with an inhibitory gating system that impedes the movement from being actually triggered while being mentally simulated [22].

Two main bodies of neuroscientific evidence support the existence of this combination of trigger signals and gating systems in the context of covert action. First, this trigger signal reflects an act of volition which is also present during motor imagery, the latter being defined as a voluntary and dynamic state where a movement is simulated without being actually executed [90,91]. Also, it has been suggested that the trigger signal used in this class of neural model is likely provided by the basal ganglia [92] which are activated during both motor imagery and actual performance [93,94]. Finally, trigger signals can also be used to control the velocity of a movement during motor imagery [95,96]. Therefore, it seems reasonable that these trigger signals would be involved in both overt and covert action. In the current model, if no intention (here provided by the PFC [90,97]) exists to mentally or actually execute a motor action, this trigger signal (the build-up of this signal would be generated by the basal ganglia [92,98] but its release mediated the PFC through fronto-basal loops [22]; these loops are not shown in Fig. 1) is zero and then the system is in an inactive state (no target is acquired to be reached). However, if there is an intention to perform overtly or covertly a motor action, this trigger signal multiplies the joint displacements that are then integrated to produce the neural command driving the joints of the arms (Fig. 1). The trigger signals were implemented as follows:

$$T_{R/L} = TG\frac{t^2}{(\lambda + t^2)} \quad (12)$$

where TG is the magnitude of the trigger signal and λ a constant that shapes this signal. Although the shape of the trigger signal used here is similar to those previously used in this class of model [54,55,86], here its implementation is different since its action is more distributed and mediated by another neural structure (here PFC). Such modified trigger signals combined with the inhibitory mechanisms described below allow this neural model to switch between overt and covert performance states.

Second, a large body of work suggests that during motor imagery the central nervous system employs inhibitory mechanisms to intercept this trigger signal, avoiding thus actually executing the movement [22,99,100]. It was previously suggested that during motor imagery, a first possible inhibitory mechanism would engage inhibitory cortical regions and another complementary mechanism would

involve cerebellum, brainstem and spinal cord [22,99–102]. Therefore, consistent with this idea, our current model includes such inhibitory mechanisms modeled as a gating system that controls the flow of motor commands from the motor/premotor regions to the peripheral effectors. Our gating system intercepts the trigger signal at a level that could be considered as cortical (the output of the inverse model is multiplied by zero) and at a relatively lower level (the output of the inverse model was multiplied by zero and the command is ready to be launched) that could be considered as brainstem and spinal cord (Fig. 1). Here the entire gating system (i.e., both gates are 'open' or 'closed' simultaneously) can be either (i) 'open' and thus both actual execution and sensory prediction occur in parallel allowing thus feedforward and feedback control or (ii) 'closed', and only the covert performance is executed.

2.3 Cortical Model for Mental Rotation and Frame of Reference Remapping

2.3.1 Mental Rotation and Frame of Reference Remapping Network

During the observation stage, the kinematics produced by the demonstrator is acquired by the visual system that sends these integrated visual inputs to the model's IPS/SPL (i.e., parietal brain regions) that in turn transforms this visual information represented from the demonstrator's allocentric into the imitator's egocentric frame of reference (i.e., remapping of demonstrator-imitator's distance, anthropometry and viewpoint). Then, remapped visual inputs are sent to the IM (located in the motor/premotor regions which are part of the frontal MNS) to generate the neural command. An efference copy of this neural drive is also sent to the forward model (located in the parietal regions which are part of the parietal MNS) to compute the sensorimotor predictions. If the trigger signals are intercepted (i.e., the gating system is closed) then the action is only observed, otherwise the triggers signals launch the actual movement and the action is imitated.

2.3.2 Architecture and Learning of the Cortical Remapping Network

Based on human neurophysiological principles, radial basis function networks were also used to model the neural architecture of the IPS/SPL brain regions [76–79]. As for the neural model described above, this model does not explicitly capture the cortical circuitry but instead represents the hypothesized functionalities. These neural networks model the transformation described below in order to map the allocentric demonstrator into the egocentric imitator frame of reference (Fig. 2) by means of modeled mental translation, rotation and scaling. The mental translation and rotation allow for the imitator to face the same perspective/orientation as the demonstrator by translating and rotating the frame of reference of the demonstrator. The scaling (or personalization) allows for the imitator remapping the observed actions in order to mentally simulate and imitate such observed actions with the imitator's own body anthropometry. By employing an orthogonal least squares learning algorithm, these neural networks learned this mapping that can be mathematically expressed as:

$$f_T = T_S(A_I, A_D) \cdot T_R(\theta_I, \theta_D) \cdot T_T(O_I, O_D) \tag{13}$$

$$T_S(u, v) = \begin{pmatrix} u_x/v_x & 0 & 0 & 0 \\ 0 & u_y/v_y & 0 & 0 \\ 0 & 0 & u_z/v_z & 0 \\ 0 & 0 & 0 & 1 \end{pmatrix} \tag{14}$$

$$T_R(u, v) = \begin{pmatrix} \cos(u-v) & -\sin(u-v) & 0 & 0 \\ \sin(u-v) & \cos(u-v) & 0 & 0 \\ 0 & 0 & 1 & 0 \\ 0 & 0 & 0 & 1 \end{pmatrix} \tag{15}$$

$$T_T(u, v) = \begin{pmatrix} 1 & 0 & 0 & u_x - v_x \\ 0 & 1 & 0 & u_y - v_y \\ 0 & 0 & 1 & u_z - v_z \\ 0 & 0 & 0 & 1 \end{pmatrix} \tag{16}$$

where $A_I, A_D \in \mathbf{R}^2$ correspond to the anthropometric data of the upper and lower arms of the imitator (I) and the demonstrator (D), $\theta_I, \theta_D \in \mathbf{R}$ represent the viewpoint angles of each agent in each frame of reference, $O_I, O_D \in \mathbf{R}^2$ represent the position vectors (or frames of reference) of each agent with respect to the global coordinate system; x,y,z denotes the Cartesian components x,y and z in the XYZ plane. It must be noted that at this stage, only rotation around the vertical z-axis was considered. $T_S(\bullet)$, $T_R(\bullet)$, and $T_T(\bullet)$ represent the scaling, rotation and translation matrices, respectively. Specifically, the angular displacement for mental rotation from the demonstrator to the imitator's viewpoint is defined as the rotation angle $\theta_I - \theta_D$. These neural networks were trained using 25 uniformly distributed spatial reference points in order to fully cover the demonstrator's workspace. After training, these sub-networks perform uniform mental visuo-spatial transformations by employing combinations of rotation, translation and scaling. These networks were trained separately from the neural networks that implement the inverse computation.

2.4 Performance Assessment of the Cortical Model

After completion of learning during which the internal representation of the inverse model of arm kinematics as well as the frame of reference mapping was encoded, the performance of the neural model was assessed by employing multiple testing situations.

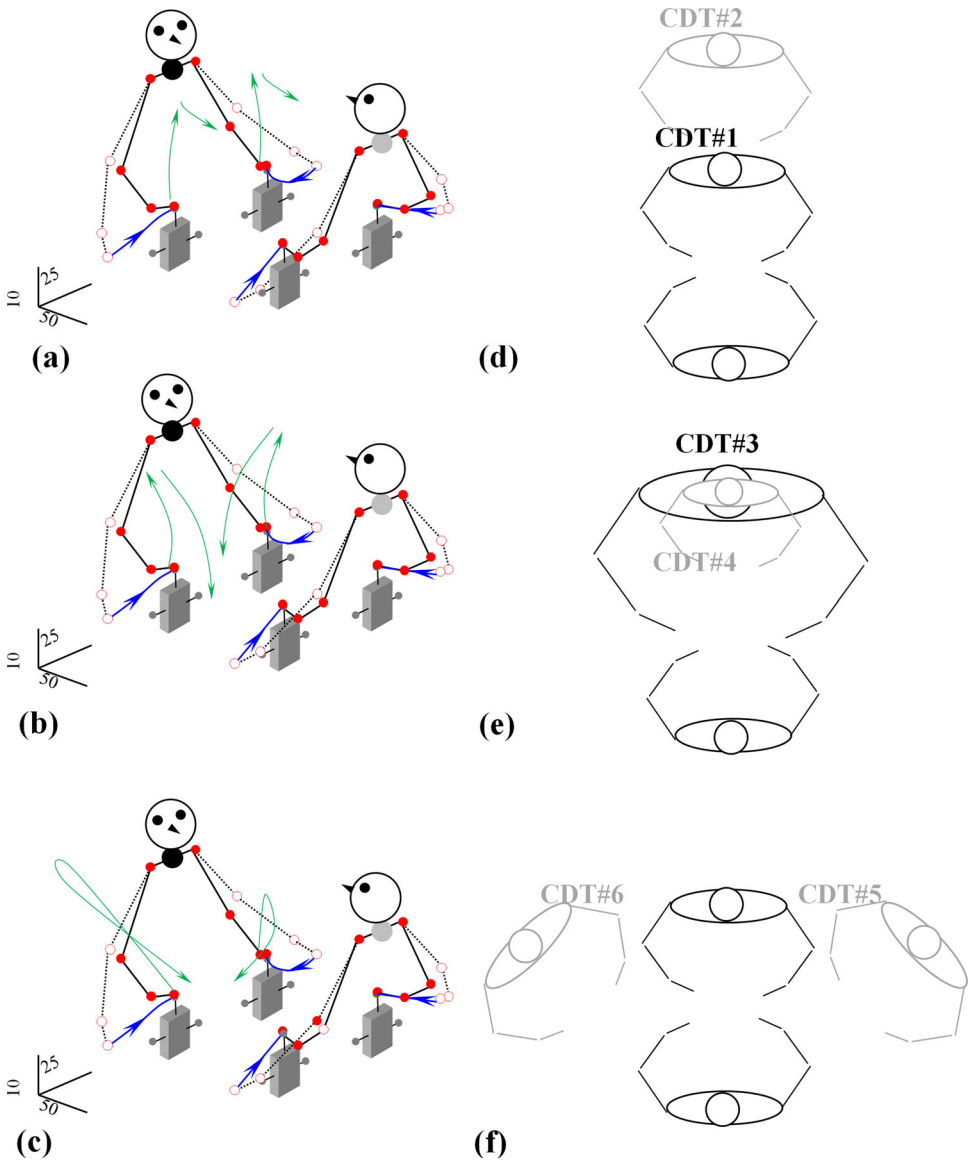

Fig. 2 Various types of movements and conditions employed to assess the imitation capabilities of the neural architecture. Three types of movement are employed: mirror (**a**), symmetric (**b**) and asymmetric (**c**). The distance (regular and far away, **d**), the anthropometry of the demonstrator (smaller and larger, **e**) and the view point (rotation of 45° and 225°, **f**) were systematically varied. The *larger black* and *gray dots* represent the neck–chest junction of the imitator (who faces the reader) and the demonstrator (showing his/her back), respectively. *CDT* condition. The *green arrows* represent the movements to imitate. The *blue lines* show the demonstrated and imitated path and include an *arrow* to illustrate the direction of the movement. (Color figure online)

First, self-intended unimanual arm performance of 3D center-out reaching movements towards multiple targets that were not specifically used for training, both during and after learning, was conducted in order to assess the control of arm reaching movements. Fourteen targets (provided by the PFC; not modeled here) were placed in order to cover a 3D workspace as was similarly done in previous human and primate reaching studies [82,103]. Additional assessment was conducted to illustrate the effects of the postural relaxation component on the behavior of the neural model, such as when the arm starts to move when initially positioned with joint angles that tend to belong to the extreme part of the range of motion.

Second, the flexibility and robustness of this neural architecture was assessed during online re-planning and in the presence of unexpected perturbations during actual self-intended unimanual reaching movements, respectively. Specifically, the online re-planning capabilities were assessed by inducing a sudden change of the target location (i.e., in movement direction). Also, the perturbation applied to the arm corresponded to an increase of 20 % of each joint angle, during both the transient and steady-state phases of the motion. The perturbations were systematically applied for each center-out reaching movement either briefly (impulse-type) or for a longer duration (step-type).

We then tested the capabilities of this neural model to mentally simulate bimanual reaching to two targets with the left and right arm (one target was presented for each limb). The task was simplified but inspired from work proposed by [104]. Here the task consisted of reaching to one target with the right arm and another one with the left arm. The neural architecture had to mentally simulate (i.e., gating sys-

tem closed) the reaching movement and predict the sensory consequence (e.g., position) in order to assess if the targets were within reaching distance. A stick was placed on the side of each arm. If the target could be reached then the simulated movement was considered as successful. However, if the arm could not attain the target, the neurocontroller could reach and use the stick in order to attain targets unreachable with the arm alone. When both targets were successfully mentally reached the entire movement sequence was launched (i.e., gating system open) and overtly executed (the high-level planning process (sequence) was not modeled here).

The capabilities of this neural architecture to generate multiple self-intended bimanual arm movements in a relatively more complex task than single reaching movements were also investigated. In this task, multiple targets were generated by a high-level planning system (the PFC, not modeled here) that provided a sequence used to move and rearrange four small boxes while covering substantially the 3D workspace.

Finally, the capability of this neural architecture to imitate movements was also examined during imitation of simple actions involving manipulation of small boxes (composed of a sequence divided into three movements) while reaching various parts of the objects (top or lateral handle). The imitation of three types of movements was systematically considered: mirror, symmetric and asymmetric movements (Fig. 2a–c). For each type of movement, three main factors were systematically varied: (i) the distance, (ii) the anthropometry, and (iii) the viewpoint (orientation) between the demonstrator and imitator (Fig. 2d–f). Specifically, the distance factor included a regular and a longer distance between the demonstrator and imitator (Fig. 2d). The factor anthropometry was varied in order to consider that the demonstrated movements were performed by a demonstrator having the same size, 20 % larger or 20 % smaller compared to the imitator (Fig. 2e). The viewpoint of the demonstrator was also changed to include a rotation of 180° between the demonstrator and imitator which in this case faced each other. Two other rotations of 45° and 225° on the right and left side of the imitator were also employed, respectively (Fig. 2f). Although this model did not aim at imitating point-to-point the observed kinematics, the imitated movements were assessed by computing the coefficients of correlation between the demonstrated and imitated displacements. Although generally the initial limb positions of the imitator and demonstrator were the same, in some cases additional changes in the initial limb positions of the imitator or the addition of perturbations (as described above) during imitated movements were also introduced to further assess the neural architecture.

3 Results

3.1 Self-Intended Unimanual and Bimanual Overt and Covert Reaching Movements

The performance error and its variability were gradually reduced throughout learning conducted in the 3D workspace (Fig. 3a). Specifically, when considering self-intended reaching movement performed towards all of the fourteen targets placed in the workspace, the average performance errors were equal to 29.11 $\pm$ 9.71, 14.34 $\pm$ 6.69 and 1.03 $\pm$ 1.56 cm for the early, middle and late learning periods, respectively. Once the learning period was over, trajectories were overall smoothed and slightly curved while the targets were accurately reached ($<$1.5 cm) (Fig. 3b). Further, the postural relaxation component of the neural model converges the arm towards more comfortable joint postures, ensuring that the joint angles will remain as much as possible in the middle of their respective range (Fig. 3c, d). Consistent with previous human studies, the kinematics results revealed that overall the displacements of the joints and of the hand were smooth and sigmoid-shaped while the joints and hand velocity profiles were generally single-peaked and bell-shaped [13,14,17,18] (Fig. 4). In addition, both joint angles and hand linear acceleration generally revealed biphasic profiles [17]. The additional assessment of the neural model when considering a sudden change of target acquisition revealed that that this neural model was able to successfully reacquire online a new target during both the transient (Fig. 5a–c) as well as during steady (Fig. 5d–f) state of the movement. These results demonstrate that this class of model provides flexibility even when controlling a highly redundant non-linear kinematics chain such as an anthropomorphic arm [54–56,86].

In addition, the assessment of robustness revealed that the cortical model was robust to various types of unexpected perturbations with substantial amplitudes (equivalent to 20 % of the current joint angle) and applied at different phases of the movement while performing self-intended reaching movements. Specifically, when both types of perturbations (impulse-type or step-type) perturbed the movement during both the transient and steady-state periods, the joints and the end-effector trajectories re-converged towards the target to reach it with an accuracy comparable (impulse-type–transient state: $<$0.05 % and steady state: $<$0.08 %; step-type:–transient state: $<$0.04 % and – steady state: $<$0.11 %) to unperturbed conditions. For example, when the effector had to reach a distant target from its initial position in the workspace, either during the transient or the steady phase of the reaching movement, the neural model was able to reach this target with a good accuracy (transient: $<$0.38 cm; steady: $<$0.39 cm) that was comparable for both unperturbed and

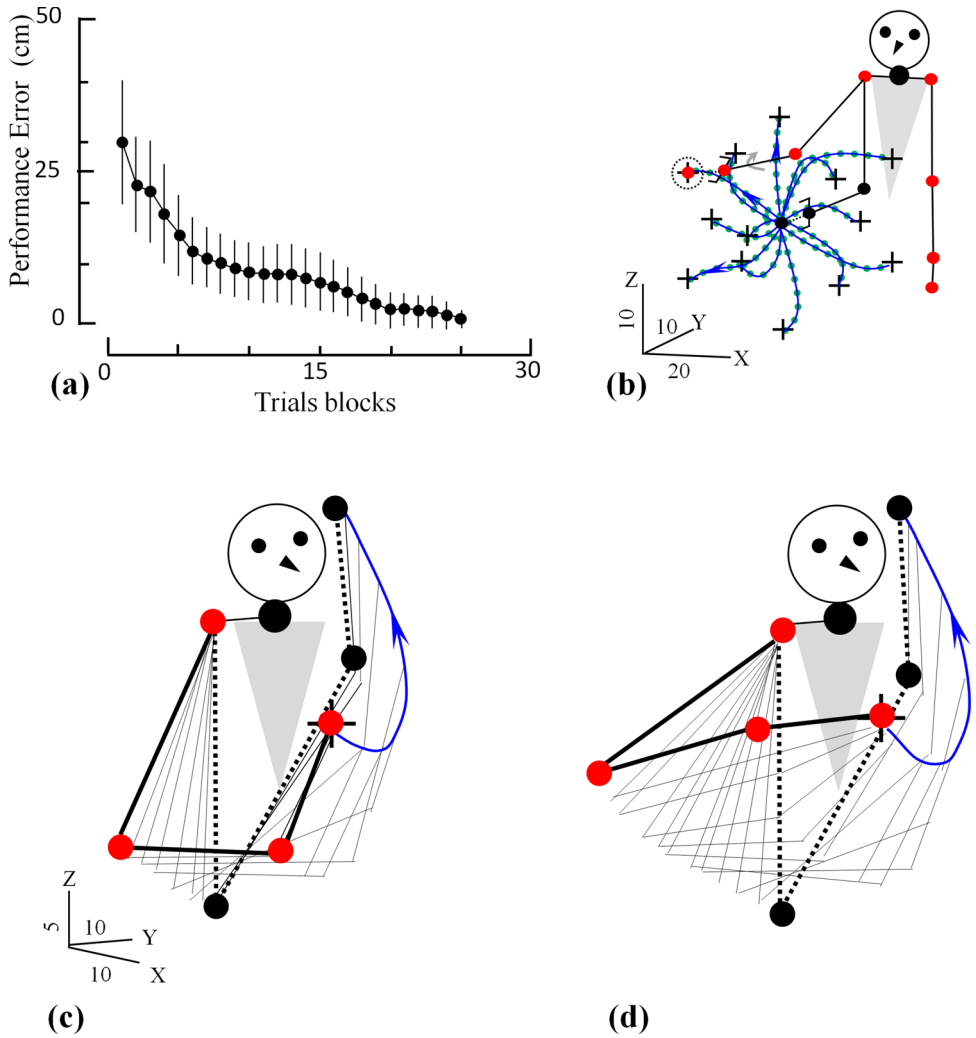

Fig. 3 Performance of unimanual actual reaching movement during the learning and performance stage. **a** Average reaching error and corresponding standard deviations throughout learning (each block represents 800 trials). **b** Actual (*solid blue lines*) and mentally simulated (*dotted green lines*) center-out reaching movements of the right arm (the *crosses* represent the spatial targets placed in the 3D workspace). A gripper illustrates the orientation of the wrist (the direction of rotation is indicated by the *gray arrow*) during the initial and final positions of the arm when reaching the target inside the *dashed circle*. The large size *black dots* represent the neck–chest junction of the performer. **c**, **d** Illustration of the effects of the postural relaxation component on the performance when movement starts from a posture with high joint flexions at the elbow and wrist. Comparison of the limb configuration during reaching when this postural component of the neural model is disabled (*left panel*) and activated (*right panel*). The *arrows* placed on the trajectories (*blue lines*; only a few of them are used in **b** for clarity) illustrate the directions of the movements. (Color figure online)

perturbed reaching conditions (Fig. 6). It must be noted that, for clarity and conciseness, these results were illustrated on the right arm; however, since an identical controller with the same properties controls the left arm, the properties mentioned above also apply to this limb.

The findings also revealed that due to its internal loops, this neurocontroller was able to mimic the consequences of the neural commands and thus mentally simulate bimanual self-intended reaching movements to reach two targets with a tool if needed (Fig. 7a–c). As such, it was possible on a simplified task to reach the targets or modify (with the help of the PFC, not modeled here) the reaching sequence in order to use a tool (stick) and re-attempt the reaching. Then, when a mentally simulated movement was successfully performed, the entire actual self-intended movement sequence was launched (Fig. 7d).

The results also revealed that the cortical model was able to generate self-initiated arm movements relatively more complex than single reaching movements by moving and rearranging small boxes while covering a large part of the workspace. Namely, by employing a particular sequence of intermediate targets (provided by the PFC, not modeled here), the neural model was able to reach them successively

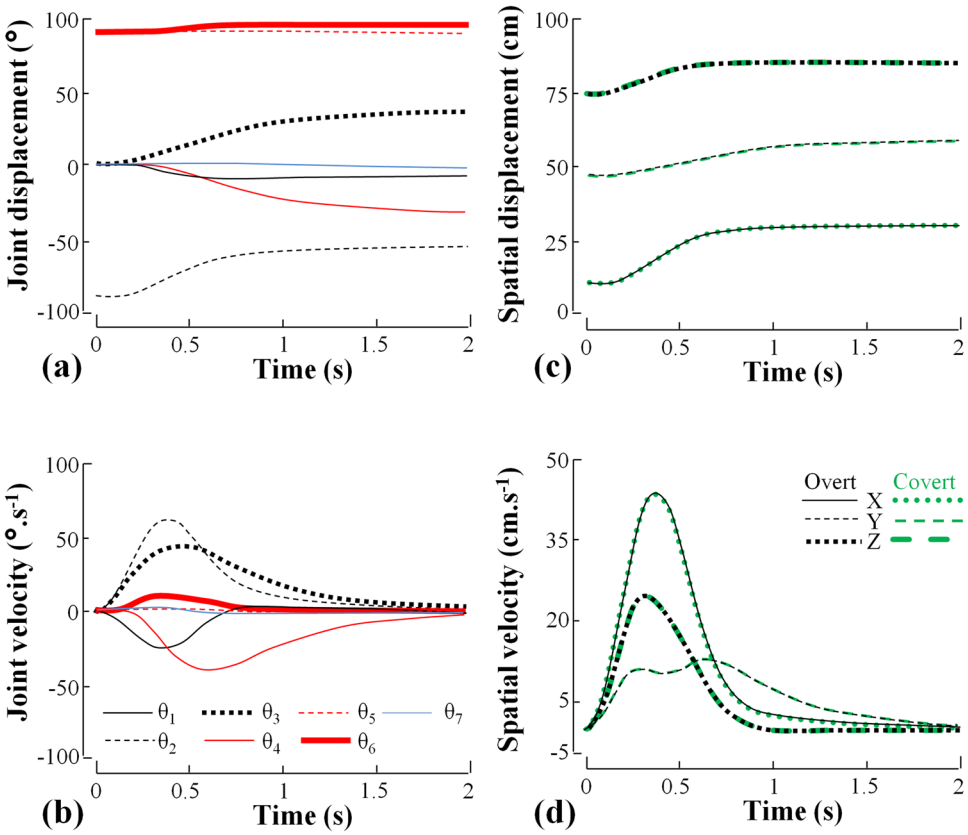

Fig. 4 Performance of unimanual reaching movement. Typical joint (*left column*) and hand (*right column*) kinematics generated by the cortical model during typical reaching movement (towards the target is indicated in Fig. 3b by a *dashed circle*). Displacement and velocity profiles are represented in the first and second row, respectively. In the *right column*, the *black* and *green lines* represent the actual and mentally simulated reaching movement. θ_1, θ_2, θ_3, θ_4, θ_5, θ_6, θ_7 represent shoulder rotation, shoulder adduction-abduction, shoulder flexion-extension, elbow flexion-extension, elbow pronation-supination, hand adduction-abduction and the hand flexion-extension, respectively. (Color figure online)

and accurately to move and rearrange these boxes in the 3D workspace (Fig. 8).

3.2 Imitated Bimanual Reaching Mirror, Symmetric and Asymmetric Movements

This neural architecture was also tested in order to assess its capacity to imitate mirror, symmetric and asymmetric movements under various visuo-spatial conditions between the imitator and the demonstrator. Overall, the neural architecture was able to imitate with good accuracy the demonstrated movements independently of the point of view of the demonstrator (Fig. 9), the difference in anthropometry (Fig. 10) and distance (Fig. 11) between the demonstrator and the imitator. In particular, the performance of the networks implementing the visuo-spatial transformation in order to remap the allo- into the ego-centric frames was very good. Specifically, the correlation coefficient between the imitated and observed displacements were superior (ranged from 0.95 to 0.98) and the error remappings were on average smaller than 3 % of the length of the limb, all type of movements and conditions considered, In addition, the neural system was able to imitate actions even when starting from different initial arm positions compared to the demonstrator (Fig. 11) or grasping the top or lateral handle (Figs. 11, 12). Finally, this neural architecture was able to imitate the same action sequence of the demonstrator even when subjected to perturbation (although the imitated kinematics were fairly different due to presence of those perturbations) (Fig. 12).

4 Discussion

Providing a robot with cognitive-motor abilities which allows it to learn bimanual arm motions by means of mental simulation and/or by observing a human perform them is widely recognized to be a challenging task, and is an area of increasingly active research. In this paper, we have proposed a neural architecture based on mental simulation theory that offers a promising approach to addressing the challenges involved. Specifically, this model offers a coherent combination of self-intended actual and mental movements as well as observed/imitated movements by modeling three fronto-parietal circuits for sensorimotor processing (visuo-spatial coordinate transformations, sensorimotor predictions, etc.). Overall, the results revealed that our model was able to perform accurate, flexible and robust 3D unimanual and bimanual reaching movements under various challenging condi-

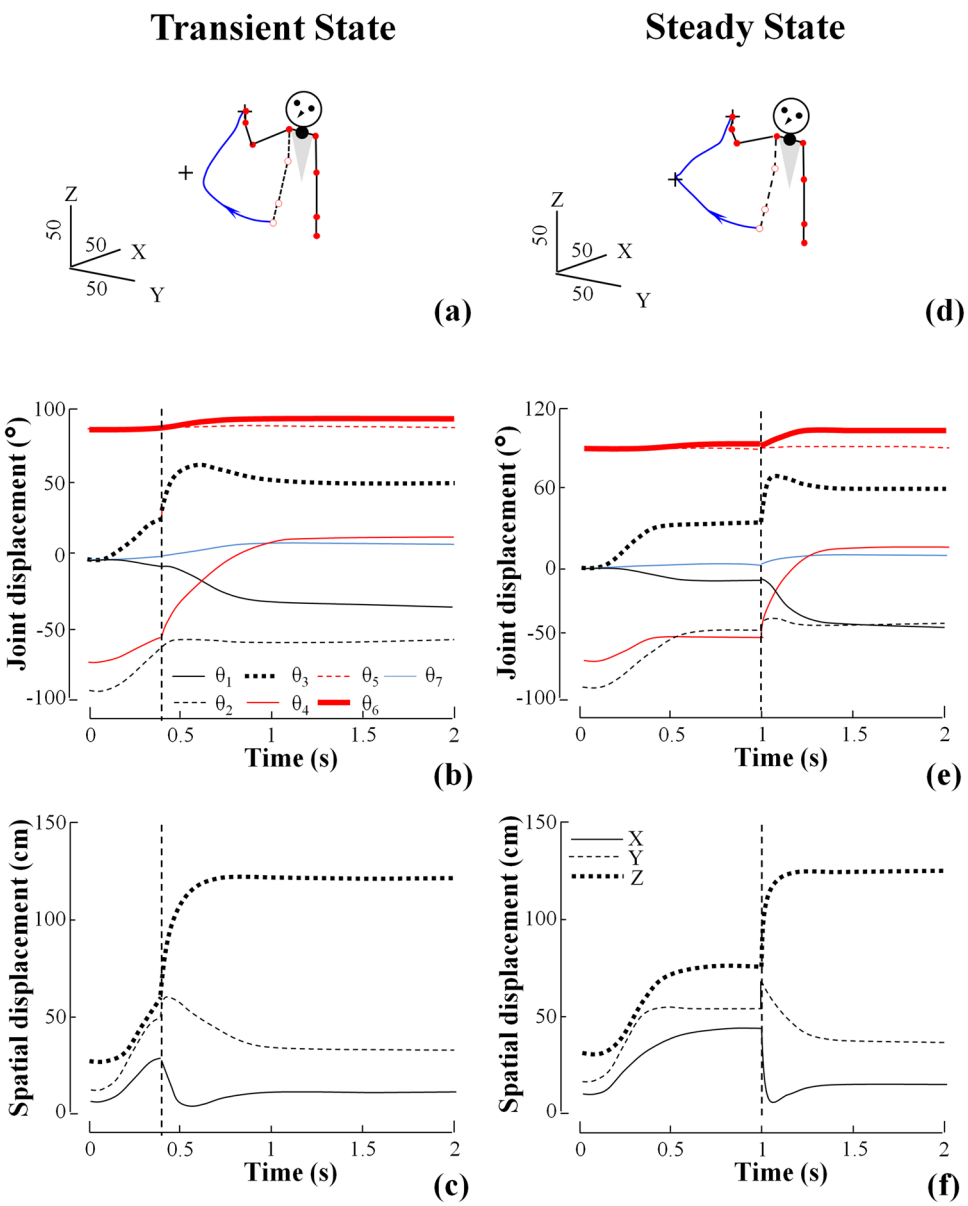

Fig. 5 Unimanual performance of the neural model during online re-planning of actual movements. Joint and hand kinematics produced by the cortical model when a sudden change of target to reach is applied during the transient (*left column*; **a**–**c**) and the steady (*right column*; **d**–**f**) state phases of motion. The first, second, and third row represents the arm configuration, the joint and hand displacement, respectively. The legend for the joint angles and the 3D displacement is the same as the ones used for Fig. 4. (Color figure online)

tions and execution modalities (self-intended mental/actual and observed/imitated movements).

4.1 Unimanual and Bimanual Actual and Mentally Simulated Reaching Performance

Our neural architecture, which is functionally inspired by the fronto-parietal cortical network, was able to perform self-intended actual and mentally simulated unimanual and bimanual movements with two anthropomorphic arms, each having seven DOFs in a 3D workspace. More specifically, our neural architecture was able to accurately reach for targets placed in a 3D workspace while (i) maintaining comfortable joint positions when the effectors tended to approach awkward postures [55] and (ii) reproducing linear and joint kinematics features similar to those observed in humans during arm reaching movements [13,14,17,18].

Generally, the neurocontroller produced sigmoid-shaped angular and linear displacements as well as smoothed single-peaked and bell-shaped angular and linear velocity profiles which are consistent with those reported from the human psychophysical literature [13,14,17,18]. This is also in agreement with other efforts that previously pointed out that this type of neural model had properties allowing for reproducing neurophysiological and psychophysical data obtained from primates and humans, respectively [54,55,86,105]. In addition, the results confirm and extend those previously obtained in an earlier version of this model applied to the far simpler problem of horizontal planar arm reaching movements with three DOFs [55], and more generally contribute

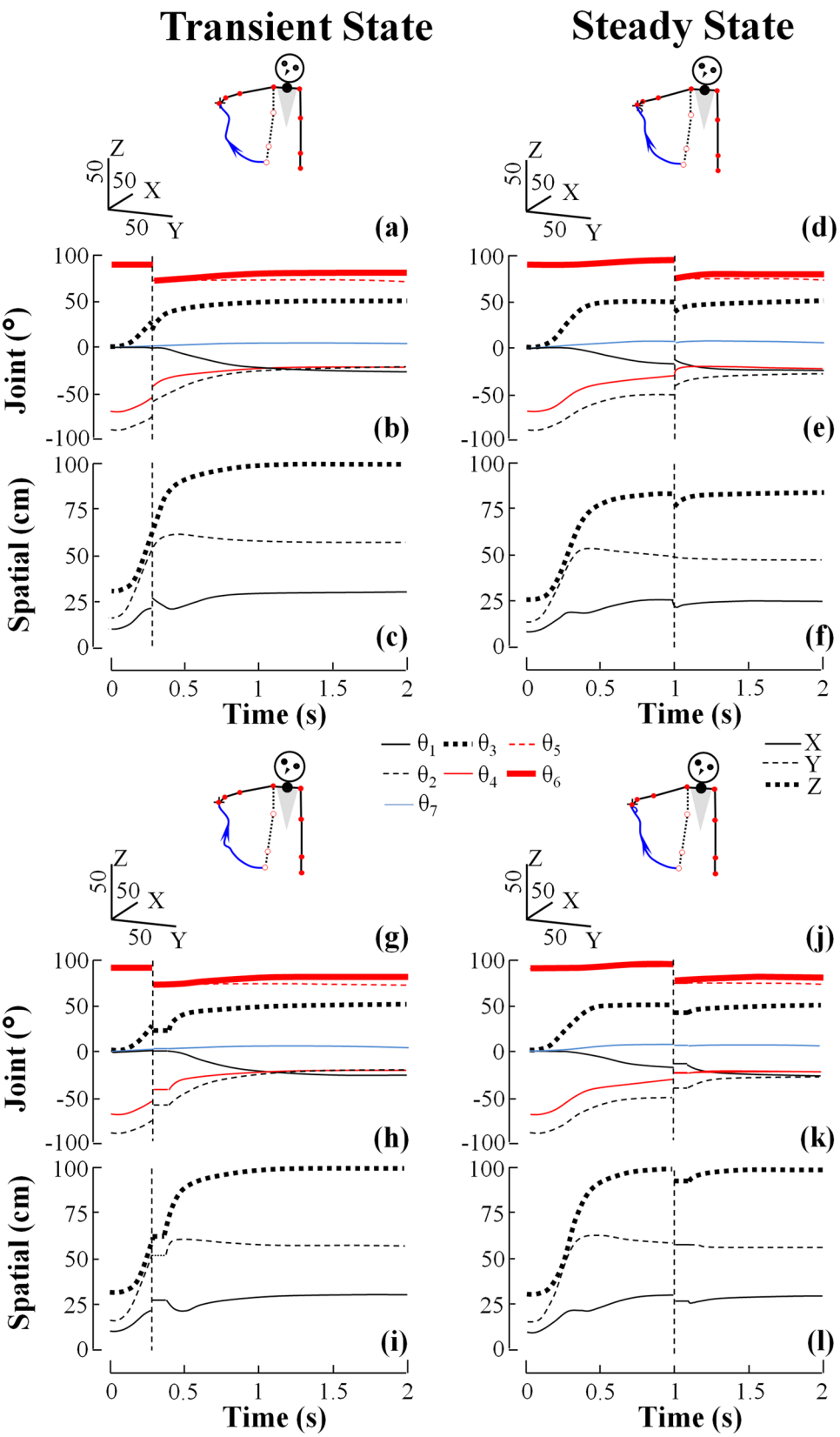

Fig. 6 Assessment of the robustness of the neural model to unexpected perturbations during unimanual actual arm movements. Responses of the cortical model to a brief (*first three rows*, **a**–**f**) and a sustained (*three last rows*, **g**–**l**) perturbation applied during the transient (*left column*) and the steady (*right column*) states of the movement. Effects of the perturbation on the joint displacements are shown in the second and fifth rows whereas the effects of the perturbation on the hand displacements are depicted in the third and sixth rows. The *dashed lines* represent when the perturbation was applied. The legend for the joint angles and the 3D displacement is the same as the ones used for Fig. 4. (Color figure online)

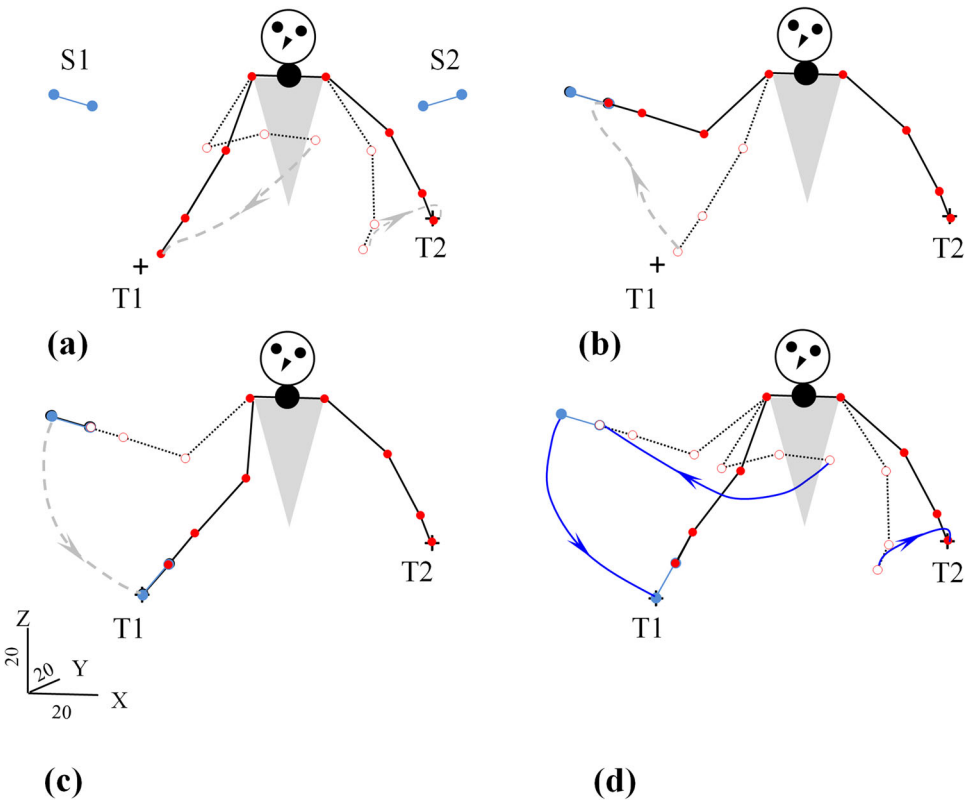

Fig. 7 Combination of actual and mentally simulated movements to execute a sequence of reaching movements to targets with or without using a tool. The two sticks (S1 and S2; in *light blue*) were placed on the side of each arm of the performer. Since in the scenario illustrated the stick S2 was not employed, for clarity this stick is only depicted in panel (**a**). **a** Mental simulation of reaching movements to the unreachable targets T1 (*right arm*) and reachable T2 (*left arm*). **b** Mental simulation of reaching movements to the stick. **c** New attempt to reach the target T1 with the tool. **d** Release of the entire actual reaching sequence to target T2 and (using the stick) to target T1. Mentally simulated and actual displacements are depicted in *dashed gray* and *solid blue lines* with *arrows* indicating the direction of movement, respectively. (Color figure online)

to further emphasizing the capabilities of this class of model when applied to upper limb (arm/finger) reaching movements [54,55,86,105,106]. Importantly, a certain degree of flexibility and robustness was exhibited by our neural architecture since it was able to re-plan online arm movements when challenged by a sudden change in target location or unexpected perturbations, to re-direct them properly towards the targets.

Beyond the production of single reaching movements, our neurocontroller was also able to generate more complex patterns of motion (moving/sorting boxes) using multiple successive reaching movements, and thus has the potential to produce more ecologically valid behaviors.

As such, this work provides new evidence that this class of neural model can perform accurate, robust (perturbation rejection) and flexible (online re-direction) relatively simple and more complex 3D reaching movement sequences with 7 DOFs effectors while generating human-like kinematics. Although this pattern of motion was generated by a sequence of targets to reach that was manually provided, in our future work this will be learned and defined by a higher-level movement sequence planner that will be incorporated in the neural architecture as part of its cognitive capabilities and enhanced autonomy when performing complex unimanual/bimanual tasks.

Our neural architecture was able to mentally simulate arm reaching movements to assess if a given target was within reaching distance or not. If not the neural system was able to mentally reach for a stick and then use this stick to assess whether the same target could be attained. Although here the task was simplified (no higher-level system was involved to generate the sequence, no reward related to the solution, no implementation of object recognition or grasping), our neural architecture was able to run the provided output of a mental simulation of reaching movements to assess environmental conditions without carrying out actual movements.

This work is consistent with but also complementary to previous efforts that proposed various cognitive architectures [11,12,53,67–70,107]. Namely, most previous modeling work related to mental simulation has been based on similar principles which include simulating the consequences of actions at the effectors and/or environmental level [11,12,53,67–70,107]. However, contrary to these previous efforts, our neurally inspired architecture enables mental simulations through specific fronto-parietal loops where the signal flow is controlled by a triggering/gating mechanism enabling actual/mental reaching performance. Also, past models were different since they did not use an internal model framework and their architecture did not combine mental simulation and action imitation/observation within the same model. Our approach is like that proposed by Nashimoto and colleagues [107] in using an internal model framework and in assuming that the IPL could incorporate

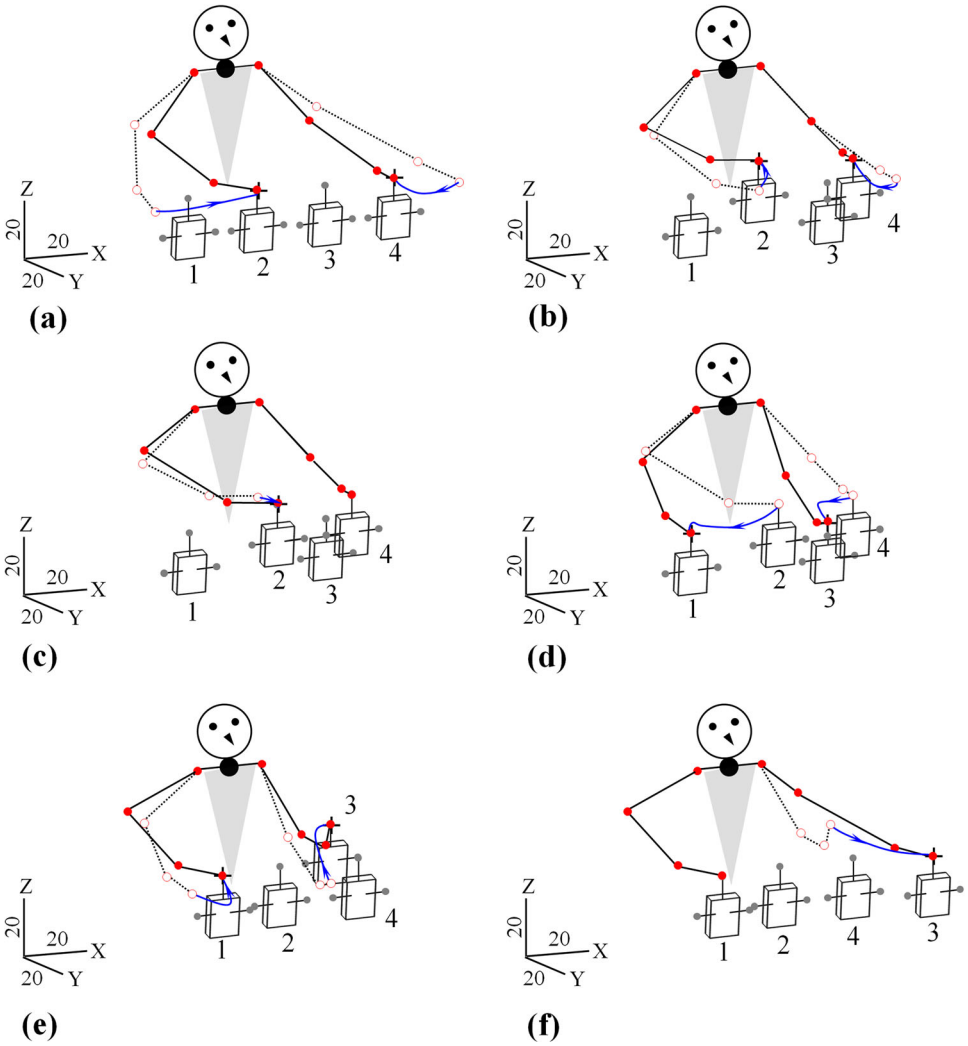

Fig. 8 Generation by the cortical model of bimanual movements to move and re-order small boxes in the 3D workspace. Multiple reaching movements were generated by the neural model (employing six set of intermediate targets; **a**–**f**). The movements are smoothly sequentially performed back to back. The performed displacements are depicted in *blue lines* with *arrows* indicating the direction of movement. (Color figure online)

forward models which are at the core of motor imagery processes for covert actions execution. However, the implementation and performance analyses of our neural model was different since (i) their learning was conducted by manipulating the robot effectors and not through a random sensorimotor exploration using a babbling stage and (ii) the arm controller was not based on inverse modeling and was not assessed in the context of perturbation and online redirection of reaching movement as is done here.

In addition, although simplified, the proposed gating mechanism is consistent with the biological hypothesis that motor commands can be inhibited at any time [108] and thus may offer to robots similar critical inhibitory abilities for safe interactions with humans. From a neurophysiological perspective, although the present gating system could be either fully open or closed, our model offers the future possibility of examining a graded gating (opened/closed to different degrees; see [109] for a possible computational implementation) that is consistent with the idea that motor inhibition could be incomplete during motor imagery resulting in residual muscular activity [110–113]. Also, it must be noted that, although the two types of inhibitory mechanisms employed here allowed for switching between overt and covert performance, they are extremely simplified and account for another complementary type of inhibition found in humans where motor inhibition is directly embedded in the imagery processes [22]. Although not being the primary goal of this work the current model offers a basis to further examine such inhibitory processes during motor imagery.

Therefore, our neural model provides a good basis for planned future extensions such as (i) adding higher-level cognitive structures (e.g., PFC) for simulating more complicated constraints/obstacles in the workspace in more complex situations; (ii) implementing and exploring motor learning resulting from the combination of self-intended mental/actual as well as observed/imitated movements mediated through various inhibitory processes in relation to other neural structures (e.g., cerebellum, PFC; basal ganglia). Those are important points since this will allow for examining

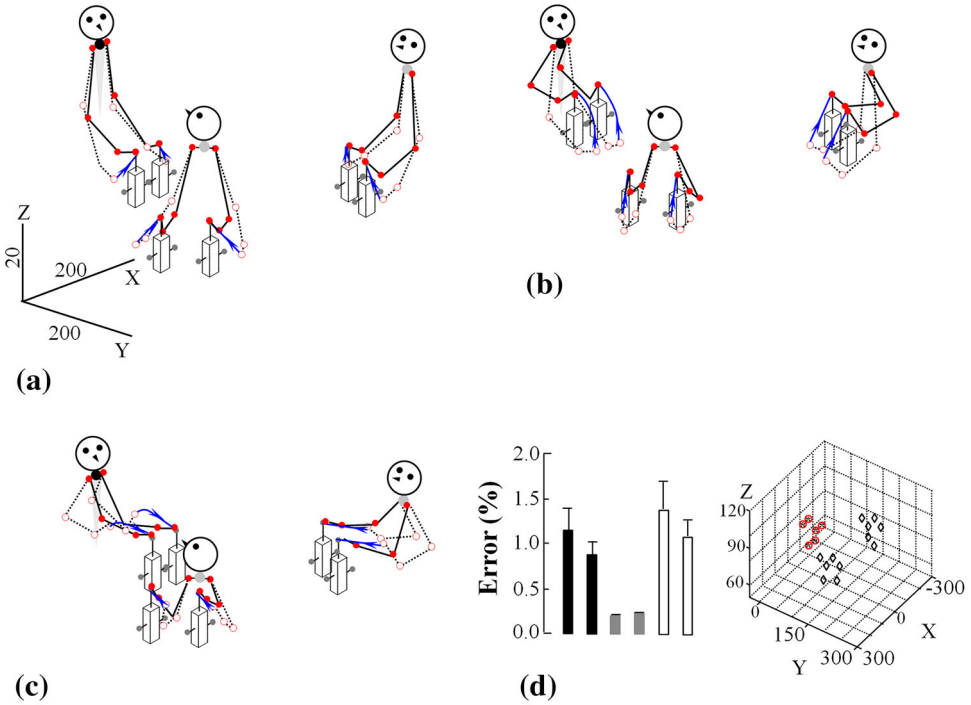

Fig. 9 Imitation of mirror movements (reach (**a**), lift (**b**) and the give (**c**) the boxes) of the boxes using their top handles. While the anthropometry between the imitator (faces the reader) and the two demonstrators is the same, compared to the imitator viewpoint, the demonstrator is placed at an angle of 45° and 225° on the right and left of the imitator. **d** The *black, gray* and *white bars* represent the average visuo-spatial transformation errors between the desired and actual rotated spatial positions of the grasped handle of each box for the three stages of the action to imitate, respectively. The *diamonds* represent the points reached by the demonstrator. The *red circles* and *black stars* represent the corresponding desired and actual rotated points with the associated error. The demonstrated and imitated displacements are depicted in *blue lines* with *arrows* indicating the direction of movement. (Color figure online)

how such movement execution modalities contribute, complement and accelerate motor learning both in humans and robots [5].

4.2 Imitation Performance

The findings show that our neural model was able to imitate correctly movements performed by a demonstrator having various anthropometries as well as located at different distances and points of view with respect to the imitator. Computationally, once the mental visuo-spatial processing such as rotation is performed, the fronto-parietal circuit can be engaged in mental simulation (i.e., observation) or actual performance (i.e., imitation) of the perceived movements. From a neuroscientific standpoint, this is consistent with previous work that indicates the presence of viewpoint dependent and independent neurons in the human mirror neuron system [66]. It is also consistent with the mental simulation theory that suggests the existence of the recruitment of a simulation network to execute mental/actual self-intended actions as well as observed/imitated actions performed by others [21]. From an applied perspective this suggests that a humanoid robot (with the proper visual processing system to extract important features) could imitate movements independently of the differences of viewpoint, distance and anthropometry with respect to the demonstrator. However, here the rotation is only performed around the vertical axis and thus it is assumed that the demonstrator trunk is positioned vertically. However, future work will extend the visuo-spatial transformation system to account for 3D rotations. Also, although our neural model can change its own movement velocity by changing its trigger signal, it cannot assess the velocity of observe movements. Fixing this would require developing new computational components to process the incoming visual stream so that it encodes the velocity of the observed movement, incorporating such information in movement imitation.

Our approach is similar to previous neural modeling work [47,48,58–63,114] since like those, our model is based on the use of internal inverse and forward models while combining mental simulation and action observation/imitation. However, one important difference is that those past biologically inspired models did not include visuospatial processes that subserve the MNS as proposed here to remap the frame of reference between the demonstrator and the imitator. To our knowledge, only few studies considered, to some extent,

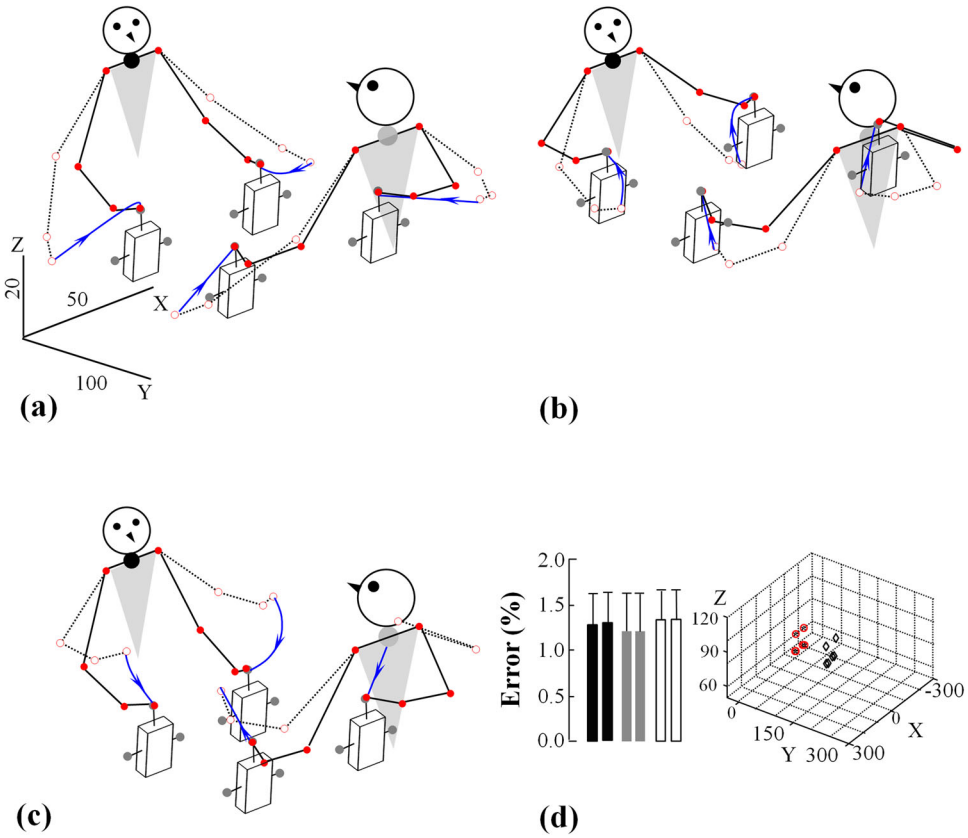

Fig. 10 Imitation of symmetric movements (reach (**a**), lift (**b**) and put back the boxes closer to each other (**c**)) of the boxes using their top handles. The anthropometry of the demonstrator is 20 % larger than that from the imitator (faces the reader). **d** The *black, gray* and *white bars* represent the average visuo-spatial transformation errors between the desired and actual rotated spatial positions of the grasped handle of each box for the three stages of the action to imitate, respectively. The *diamonds* represent the points reached by the demonstrator. The *red circles* and *black stars* represent the corresponding desired and actual rotated points with associated errors. The demonstrated and imitated displacements are depicted in *blue lines* with *arrows* indicating the direction of movement. (Color figure online)

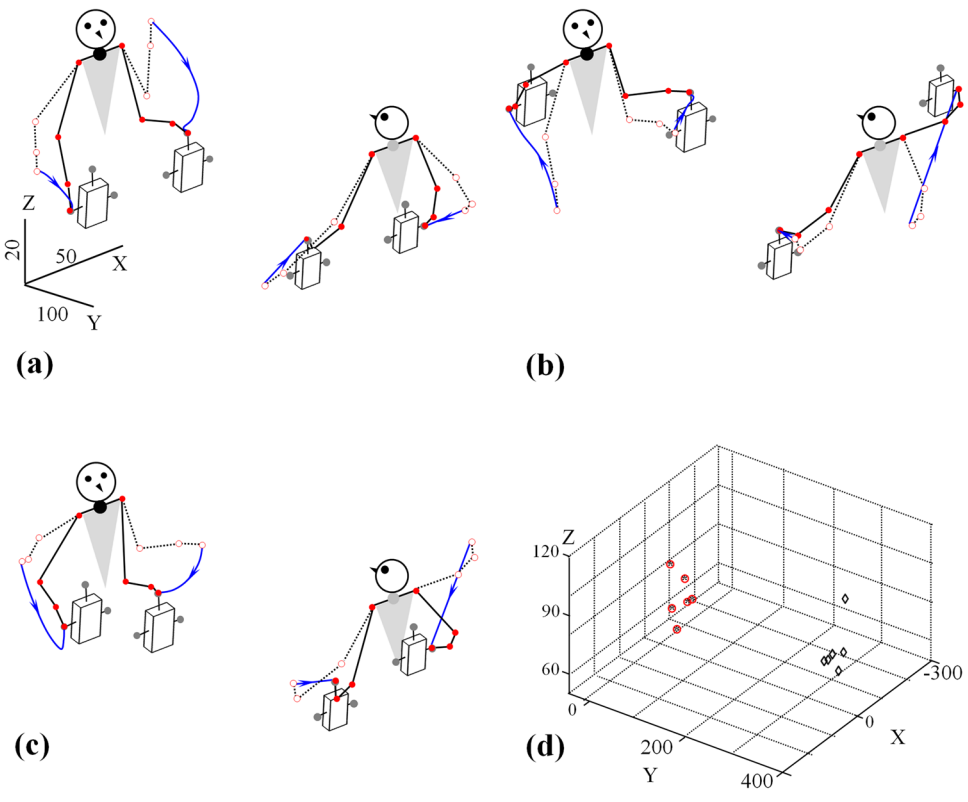

Fig. 11 Imitation of asymmetric movements (reach (**a**), lift with asymmetric movements (**b**) and place the boxes at a place different from their initial position (**c**)) for moving boxes using their top and lateral handles. The anthropometry of the demonstrator and imitator is the same. The imitator (faces the reader) starts with a different initial limb position compared to that used by the demonstrator and the distance between both of them is larger. **d** The *diamonds* represent the points reached by the demonstrator. The *red circles* and *black* stars represent the corresponding desired and actual rotated spatial positions of the grasped handle, respectively. The demonstrated and imitated displacements are depicted in *blue lines* with *arrows* indicating the direction of movement. (Color figure online)

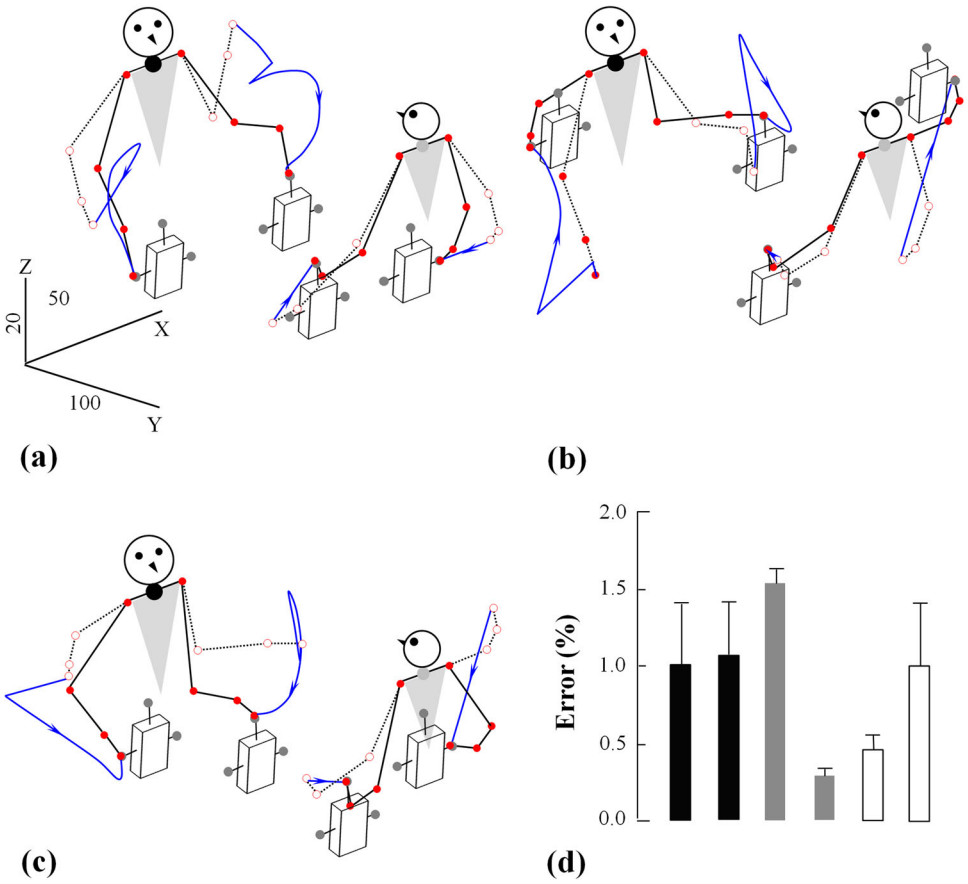

Fig. 12 Imitation of asymmetric movements (reach (**a**), lift with asymmetric movements (**b**) and place the boxes at a place different from their initial position (**c**)) for moving boxes using their top and lateral handles. The anthropometry of the demonstrator is 20 % smaller than that from the imitator. The imitator (faces the reader) starts with a different initial limb position compared to that used by the demonstrator and its movements are subjected to sudden perturbations at each stage of the imitation. **d** The *black, gray* and *white bars* represent the corresponding average average visuo-spatial transformation errors between the desired and actual rotated spatial positions of the grasped handle of each box for the three stages of the action to imitate, respectively. The demonstrated and imitated displacements are depicted in *blue lines* with *arrows* indicating the direction of movement. (Color figure online)

such transformations. For instance, although it was not a primary component, Billard and colleagues [60] included this transformation in their neural architecture for action observation/imitation. However, their model was different from ours since the visuomotor transformation did not learn to remap the anthropometry, distance and orientation of the observer and was not based on an internal model framework. Also, Lopes and colleagues [62] implemented such transformations but their proposed solution was purely mathematical without any biology relevance. In addition, none of these two past neural models integrated mental simulation in their architecture. More recently, and although it was not the primary focus of the study, Ari and colleagues [63] showed that their neural model was able to handle small changes limited to $\pm 15°$ between the imitator and the demonstrator. However, the authors suggested that with larger variations visuo-spatial processes such as "mental rotation" should be considered.

It should be noted that although the kinematic correspondence between imitated and demonstrated movements was generally good, here the aim was not to imitate the demonstrator's trajectory point-to-point per-se but rather to re-map the relevant contact points (e.g., top handle, lateral handle) that can be considered as sub-goals of an action or task. When an imitated movement was either started from different initial positions or subjected to unexpected perturbations, the neural model was still able to reach with its arms the targets remapped into its frame of reference. Under such conditions, the kinematics trajectory of course differed from the one demonstrated; however, the neural system was still able to reproduce the observed actions, such as moving the boxes in the workspace as shown by the demonstrator. Thus, although this is only a first step, this approach is consistent with the idea that movement observation/imitation is not related only to the kinematics of the demonstrator per-se but also to higher-level goals. This view is in agreement with other models of learning by demonstration [5,38,50,51,115]. In summary, the present neural architecture complements these previous efforts by proposing a unified framework that incorporates mental/actual self-intended and observed/imitated bimanual movements in a single framework along with spatio-visual mental transformations applied to the environment.

4.3 Limitations of the Model and Future Work

At present our cortical network model does not include any component accounting for biomechanical dynamics (e.g., gravity, inertia), which is an important limitation. Our future work will solve this problem by focusing on the dynamics of the arms. This will be done by incorporating a model of cerebellar pathways that has been previously considered to

encode internal models of the inverse and forward dynamics [57,116].

Another important extension will be the design of a higher cognitive level via a model of PFC that includes higher cognitive functions, thus allowing an enhanced flow of information between higher and lower levels consistent with the human prefrontal–parietal network. Specifically, such an addition will allow the expanded architecture to simulate a set of self-intended mental or observed movements at a lower level (i.e., output of the forward model, corresponding to the parietal brain regions) that could be transmitted to a higher level cognitive structure such as the PFC. These predictions would be integrated by the PFC in order to (i) recognize or predict the goal of the observed actions (action understanding) and (ii) allow for inhibitory control and a higher re-planning level such as an entire sequence of actions. Such interactions between higher and lower levels will also further focus on combining learning using self-intended movements, employing imitation in order to further explore accelerating motor learning, and providing increased robustness during decision making and carrying out actions in changing environments as observed in humans. Such mental simulations combined with imitation/observation capabilities in robots would allow them to produce more human-like behavior while learning from humans, and to improve human–machine interactions, including when human patients interact with assistive or rehabilitative machine in clinical settings.

Finally, future work will assess the capability of our neural architecture to effectively control a physical robotic arm in a real world environment. Interestingly, previous work which employed a similar neural architecture was able to successfully control an actual humanoid robotic arm with five DOFs [106] and a finger that included mechanical coupling of the two last joints [105]. Over the long term this research can contribute to developing a neurally inspired control system incorporating cognitive-motor processing more similar to humans in order to provide a platform to examine human performance as well as to enable adaptive, robust and flexible control of dexterous robotic upper extremities.

Acknowledgments This research was supported by the Office of Naval Research (ONR; N000141310597), USA.

References

1. Shadmehr R (2005) The computational neurobiology of reaching and pointing: a foundation for motor learning. MIT, Cambridge
2. Kamper DG, Cruz EG, Siegel MP (2003) Stereotypical fingertip trajectories during grasp. J Neurophysiol 90(6):3702–3710. doi:10.1152/jn.00546.2003
3. Billard AG, Calinon S, Guenter F (2006) Discriminative and adaptive imitation in uni-manual and bi-manual tasks. Robot Auton Syst 54(5):370–384. doi:10.1016/j.robot.2006.01.007
4. Cuijpers RH, van Schie HT, Koppen M, Erlhagen W, Bekkering H (2006) Goals and means in action observation: a computational approach. Neural Netw 19(3):311–322. doi:10.1016/j.neunet.2006.02.004
5. Billard A, Calinon S, Dillmann R, Schaal S (2008) Robot programming by demonstration. In: Siciliano B, Khatib O (eds) Springer handbook of robotics. Springer, Berlin, pp 1371–1394. Retrieved from http://www.springerlink.com/index/10.1007/978-3-540-30301-5_60
6. Nicolescu M, Mataric M (2009) Task learning through imitation and human–robot interaction. In: Dautenhahn K, Nehaniv C (eds) Models and mechanisms of imitation and social learning in robots, humans and animals. Cambridge University Press, Cambridge, pp 407–424
7. Argall BD, Chernova S, Veloso M, Browning B (2009) A survey of robot learning from demonstration. Robot Auton Syst 57(5):469–483. doi:10.1016/j.robot.2008.10.024
8. Umar Suleman M, Awais MM (2011) Learning from demonstration in robots: experimental comparison of neural architectures. Robot Comput Integr Manuf 27(4):794–801. doi:10.1016/j.rcim.2010.10.010
9. Tani J (2007) On the interactions between top-down anticipation and bottom-up regression. Front Neurorobotics 1. doi:10.3389/neuro.12.002.2007
10. Mohan V, Morasso P, Metta G, Kasderidis S (2011) Actions and Imagined Actions in Cognitive Robots. In: Cutsuridis V, Hussain A, Taylor JG (eds) Perception–action cycle. Springer, New York, pp 539–572. Retrieved from http://www.springerlink.com/index/10.1007/978-1-4419-1452-1_17
11. Toussaint M (2006) A sensorimotor map: modulating lateral interactions for anticipation and planning. Neural Comput 18(5):1132–1155. doi:10.1162/089976606776240995
12. Shanahan M (2006) A cognitive architecture that combines internal simulation with a global workspace. Conscious Cogn 15(2):433–449. doi:10.1016/j.concog.2005.11.005
13. Morasso P (1981) Spatial control of arm movements. Exp Brain Res 42(2). doi:10.1007/BF00236911
14. Abend W, Bizzi E, Morasso P (1982) Human arm trajectory formation. Brain 105(Pt 2):331–348
15. Flash T, Hogan N (1985) The coordination of arm movements: an experimentally confirmed mathematical model. J Neurosci 5(7):1688–1703
16. Nakano E, Imamizu H, Osu R, Uno Y, Gomi H, Yoshioka T, Kawato M (1999) Quantitative examinations of internal representations for arm trajectory planning: minimum commanded torque change model. J Neurophysiol 81(5):2140–2155
17. Gordon J, Ghilardi MF, Ghez C (1994) Accuracy of planar reaching movements. I. Independence of direction and extent variability. Exp Brain Res 99(1):97–111
18. Gentili R, Han CE, Schweighofer N, Papaxanthis C (2010) Motor learning without doing: trial-by-trial improvement in motor performance during mental training. J Neurophysiol 104(2):774–783. doi:10.1152/jn.00257.2010
19. Wolpert DM, Miall RC (1996) Forward models for physiological motor control. Neural Netw 9(8):1265–1279
20. Wolpert DM, Doya K, Kawato M (2003) A unifying computational framework for motor control and social interaction. Philos Trans R Soc Lond B 358(1431):593–602. doi:10.1098/rstb.2002.1238
21. Jeannerod M (2001) Neural simulation of action: a unifying mechanism for motor cognition. Neuro Image 14(1 Pt 2):S103–109. doi:10.1006/nimg.2001.0832
22. Guillot A, Di Rienzo F, Macintyre T, Moran A, Collet C (2012) Imagining is not doing but involves specific motor commands: a review of experimental data related to motor inhibi-

tion. Front Hum Neurosci 6(247):2012. doi:10.3389/fnhum.2012.00247.eCollection
23. Munzert J, Lorey B, Zentgraf K (2009) Cognitive motor processes: the role of motor imagery in the study of motor representations. Brain Res Rev 60(2):306–326. doi:10.1016/j.brainresrev.2008.12.024
24. Bakker M, de Lange FP, Stevens JA, Toni I, Bloem BR (2007) Motor imagery of gait: a quantitative approach. Exp Brain Res 179(3):497–504. doi:10.1007/s00221-006-0807-x
25. Decety J, Jeannerod M (1995) Mentally simulated movements in virtual reality: does Fitts's law hold in motor imagery? Behav Brain Res 72(1–2):127–134
26. Papaxanthis C, Pozzo T, Kasprinski R, Berthoz A (2003) Comparison of actual and imagined execution of whole-body movements after a long exposure to microgravity. Neurosci Lett 339(1):41–44
27. Papaxanthis C, Schieppati M, Gentili R, Pozzo T (2002) Imagined and actual arm movements have similar durations when performed under different conditions of direction and mass. Exp Brain Res 143(4):447–452. doi:10.1007/s00221-002-1012-1
28. Miall RC (2003) Connecting mirror neurons and forward models. Neuroreport 14(17):2135–2137. doi:10.1097/01.wnr.0000098751.87269.77
29. Carr L, Iacoboni M, Dubeau M-C, Mazziotta JC, Lenzi GL (2003) Neural mechanisms of empathy in humans: a relay from neural systems for imitation to limbic areas. Proc Natl Acad Sci USA 100(9):5497–5502. doi:10.1073/pnas.0935845100
30. Iacoboni M, Koski LM, Brass M, Bekkering H, Woods RP, Dubeau MC, Mazziotta JC, Rizzolatti, G. (2001) Reafferent copies of imitated actions in the right superior temporal cortex. Proc Natl Acad Sci USA 98(24):13995–13999. doi:10.1073/pnas.241474598
31. Gallese V, Fadiga L, Fogassi L, Rizzolatti G (1996) Action recognition in the premotor cortex. Brain 119(Pt 2):593–609
32. Rizzolatti G, Fogassi L, Gallese V (2001) Neurophysiological mechanisms underlying the understanding and imitation of action. Nat Rev Neurosci 2(9):661–670. doi:10.1038/35090060
33. Pfeifer R, Lungarella M, Iida F (2012) The challenges ahead for bio-inspired 'soft' robotics, vol 55(11). ACM, New York, pp 76–87. doi:10.1145/2366316.236633534
34. Diftler MA, Mehling JS, Abdallah ME, Radford NA, Bridgwater LB, Sanders AM, Askew RS, Linn DM, Yamokoski JD, Permenter FA, Hargrave BK, Platt R, Savely RT, Ambrose RO (2011) Robonaut 2—the first humanoid robot in space. In: IEEE international conference on robotics and automation, Shanghai, China, 9–13 May 2011, pp 2178–2183
35. Bullock IM, Ma RR, Dollar AM (2013) A hand-centric classification of human and robot dexterous manipulation. IEEE Trans Haptics 6(2):129–144. doi:10.1109/TOH.2012.53
36. Ruini F, Apel JS, Morse AF, Cangelosi A, Ellis R, Goslin J, Fische MH (2012) Towards a Biologically-inspired Cognitive Architecture for Short-Term Memory in Humanoid Robots. In: Advances in autonomous robotics. Lecture Notes in Computer Science, vol 7429. Springer, Berlin, pp 453–454. doi:10.1007/978-3-642-32527-4_55
37. Diamond A, Holland OE (2014) Reaching control of a full-torso, modelled musculoskeletal robot using muscle synergies emergent under reinforcement learning. Bioinspir Biomim 9:016015. doi:10.1088/1748-3182/9/1/016015
38. Pook PK, Ballard DH (1993) Recognizing teleoperated manipulations. IEEE Comput. Soc. Press, pp 578–585. doi:10.1109/ROBOT.1993.291896
39. Nehaniv CL, Ab HA, Dautenhahn K (1999) Of hummingbirds and helicopters: an algebraic framework for interdisciplinary studies of imitation and its applications. In: Demiris J, Birk A (eds) Interdisciplinary approaches to robot learning. World Scientific Press, Singapore, pp 136–161
40. Tso SK, Liu KP (1996) Hidden Markov model for intelligent extraction of robot trajectory command from demonstrated trajectories. IEEE, pp 294–298. doi:10.1109/ICIT.1996.601593
41. Shon AP, Grochow K, Rao RPN (2005) Robotic imitation for human motion capture using gaussian processes. IEEE, pp 129–134. doi:10.1109/ICHR.2005.1573557
42. Aleotti J, Caselli S (2005) Trajectory clustering and stochastic approximation for robot programming by demonstration. IEEE, pp 1029–1034. doi:10.1109/IROS.2005.1545365
43. Jäkel R, Schmidt-Rohr SR, Rühl SW, Kasper A, Xue Z, Dillmann R (2012) Learning of planning models for dexterous manipulation based on human demonstrations. Int J Soc Robot 4(4):437–448. doi:10.1007/s12369-012-0162-y
44. Mellmann H, Cotugno G (2011) Dynamic motion control: adaptive bimanual grasping for a humanoid robot. Fundam Inf 112:89–101
45. Lee J, Chang P, Jamisola R (2013) Relative Impedance control for dual-arm robots performing asymmetric bimanual tasks. In: IEEE transactions on industrial electronics 1-1. doi:10.1109/TIE.2013.2266079
46. Hersch M, Billard AG (2008) Reaching with multi-referential dynamical systems. Auton Robots 25(1–2):71–83. doi:10.1007/s10514-007-9070-7
47. Mohan V, Morasso P, Metta G, Sandini G (2009) A biomimetic, force-field based computational model for motion planning and bimanual coordination in humanoid robots. Auton Robots 27(3):291–307. doi:10.1007/s10514-009-9127-x
48. Oztop E, Lin L, Kawato M, Cheng G (2006) Dexterous skills transfer by extending human body schema to a robotic hand. IEEE, pp 82–87. doi:10.1109/ICHR.2006.321367
49. Oztop E, Kawato M, Arbib M (2006) Mirror neurons and imitation: a computationally guided review. Neural Netw 19(3):254–271. doi:10.1016/j.neunet.2006.02.002
50. Demiris Y, Hayes G (2002) Imitation as a dual-route process featuring predictive and learning components: a biologically-plausible computational model. In: Dautenhahn K, Nehaniv C (eds) Imitation in animals and artifacts. MIT, Cambrige, pp 327–361
51. Demiris Y, Khadhouri B (2006) Hierarchical attentive multiple models for execution and recognition of actions. Robot Auton Syst 54(5):361–369. doi:10.1016/j.robot.2006.02.003
52. Sauser E, Billard A (2006) Biologically inspired multimodal integration: interferences in a human–robot interaction game. IEEE, pp 5619–5624. doi:10.1109/IROS.2006.282283
53. Toussaint M (2004) Learning a world model and planning with a self-organizing dynamic neural system. In: Thrun S, Saul LK, Schölkopf B (eds) Advances in neural information processing systems 16. MIT, Cambridge, pp 929–936
54. Bullock D, Grossberg S, Guenther FH (1993) A self-organizing neural model of motor equivalent reaching and tool use by a multijoint arm. J Cogn Neurosci 5(4):408–435. doi:10.1162/jocn.1993.5.4.408
55. Guenther FH, Micci Barreca D (1997) Neural models for flexible control of redundant systems. In: Morasso PG, Sanguineti V (eds) Self-organization, computational maps, and motor control. Elsevier, North Holland, pp 383–421
56. Fiala JC (1995) Neural network models of motor timing and coordination. PhD dissertation, Cognitive & Neural Systems Department, Boston University, Boston
57. Gentili RJ, Papaxanthis C, Ebadzadeh M, Eskiizmirliler S, Ouanezar S, Darlot C (2009) Integration of gravitational torques in cerebellar pathways allows for the dynamic inverse computation of vertical pointing movements of a robot arm. PLoS One 4(4):e5176. doi:10.1371/journal.pone.0005176

58. Bonaiuto J, Arbib MA (2010) Extending the mirror neuron system model, II: what did I just do? A new role for mirror neurons. Biol Cybern 102:341–359
59. Bonaiuto J, Rosta E, Arbib MA (2007) Extending the mirror neuron system model, I. Audible actions and invisible grasps. Biol Cybern 96:9–38
60. Billard A, Mataric MJ (2001) Learning human arm movements by imitation: evaluation of a biologically inspired connectionist architecture. Robot Auton Syst 37:145–160
61. Demiris Y, Johnson M (2003) Distributed, predictive perception of actions: a biologically inspired robotics architecture for imitation and learning. Connect Sci 15(4):231–243
62. Lopes M, Santos-Victor J (2005) Visual learning by imitation with motor representations. IEEE Trans Syst Man Cybern B 35(3):438–449
63. Arie H, Arakaki T, Sugano S, Tani J (2012) Imitating others by composition of primitive actions: a neuro-dynamic model. Robot Auton Syst 60:729–741. doi:10.1016/j.robot.2011.11.005
64. Roy D, Hsiao KY, Mavridis N (2004) Mental imagery for a conversational robot. IEEE Trans Syst Man Cybern B 34(3):1374–1383. doi:10.1109/TSMCB.2004.823327
65. Nehaniv CL, Dautenhahn K (2002) The correspondence problem. Imitation in animals and artifacts. MIT, Cambridge, pp 41–61
66. Caggiano V, Fogassi L, Rizzolatti G, Pomper JK, Thier P, Giese MA, Casile A (2011) View-based encoding of actions in mirror neurons of area f5 in macaque premotor cortex. Curr Biol 21(2):144–148. doi:10.1016/j.cub.2010.12.022
67. Chrisley RL (1990) Cognitive map construction and use: a parallel distributed processing approach. In: Touretzky D, Hinton G, Sejnowski T (eds) The proceedings of the 1990 connectionist models summer school. Morgan Kaufmann, San Mateo
68. Tani J (1996) Model-based learning for mobile robot navigation from the dynamical systems perspective. IEEE Trans Syst Man Cybern B 26(3):421–436. doi:1083-4419(96)03240-2
69. Cassimatisa NL, Trafton JG, Bugajska MD, Schultz AC (2004) Integrating cognition, perception and action through mental simulation in robots. Robot Auton Syst 49:13–23. doi:10.1016/j.robot.2004.07.014
70. Ziemke T, Jirenhed DA, Hesslow G (2005) Internal simulation of perception: a minimal neuro-robotic model. Neurocomputing 68:85–104
71. Hauber W (1998) Involvement of basal ganglia transmitter systems in movement initiation. Prog Neurobiol 56(5):507–540
72. Burgess PW, Dumontheil I, Gilbert SJ (2007) The gateway hypothesis of rostral prefrontal cortex (area 10) function. Trends Cogn Sci 11(7):290–298. doi:10.1016/j.tics.2007.05.004
73. Wolpert DM, Goodbody SJ, Husain M (1998) Maintaining internal representations: the role of the human superior parietal lobe. Nat Neurosci 1(6):529–533. doi:10.1038/2245
74. Blakemore S-J, Sirigu A (2003) Action prediction in the cerebellum and in the parietal lobe. Exp Brain Res 153(2):239–245. doi:10.1007/s00221-003-1597-z
75. Gentili R, Papaxanthis C, Pozzo T (2006) Improvement and generalization of arm motor performance through motor imagery practice. Neuroscience 137(3):761–772. doi:10.1016/j.neuroscience.2005.10.013
76. Buneo CA, Andersen RA (2006) The posterior parietal cortex: sensorimotor interface for the planning and online control of visually guided movements. Neuropsychologia 44(13):2594–2606. doi:10.1016/j.neuropsychologia.2005.10.011
77. Grefkes C, Fink GR (2005) The functional organization of the intraparietal sulcus in humans and monkeys. J Anat 207(1):3–17. doi:10.1111/j.1469-7580.2005.00426.x
78. Oh H, Gentili RJ, Reggia JA, Contreras-Vidal JL (2011) Learning of spatial relationships between observed and imitated actions allows invariant inverse computation in the frontal mirror neuron system. In: Proceedings of annual international conference of the IEEE Engineering in Medicine and Biology Society, pp 4183–4186. doi:10.1109/IEMBS.2011.6091038
79. Oh H, Gentili RJ, Reggia JA, Contreras-Vidal JL (2012) Modeling of visuospatial perspectives processing and modulation of the fronto-parietal network activity during action imitation. In: Proceedings of annual international conference of the IEEE Engineering in Medicine and Biology Society, pp 2551–2554. doi:10.1109/EMBC.2012.6346484
80. Marconi B, Genovesio A, Battaglia-Mayer A, Ferraina S, Squatrito S, Molinari M, ... Caminiti R (2001) Eye-hand coordination during reaching. I. Anatomical relationships between parietal and frontal cortex. Cereb Cortex 11(6):513–527
81. Gharbawie OA, Stepniewska I, Kaas JH (2011) Cortical connections of functional zones in posterior parietal cortex and frontal cortex motor regions in new world monkeys. Cereb Cortex 21(9):1981–2002. doi:10.1093/cercor/bhq260
82. Georgopoulos AP, Schwartz AB, Kettner RE (1986) Neuronal population coding of movement direction. Science 233(4771):1416–1419
83. Ito M (2013) Error detection and representation in the olivocerebellar system. Front Neural Circuits 7:1. doi:10.3389/fncir.2013.00001 eCollection 2013
84. Liégeois A (1977) Automatic supervisory control of the configuration and behavior of multibody mechanisms. IEEE Trans Syst Man Cybern 7(12):868–871. doi:10.1109/TSMC.1977.4309644
85. Baillieul J, Hollerbach, Brockett RW (1984) Programming and control of kinematically redundant manipulators. In: IEEE conference on decision and control, December 1984, pp 768–774. doi:10.1109/CDC.1984.272110
86. Molina-Vilaplana J, Feliu-Batlle J, López-Coronado J (2007) A modular neural network architecture for step-wise learning of grasping tasks. Neural Netw 20(5):631–645. doi:10.1016/j.neunet.2007.02.003
87. Poggio T, Girosi F (1989) A theory of networks for approximation and learning. AI Memo No. 1140. MIT, Cambridge
88. Hartenberg RS, Denavit J (1964) Kinematic synthesis of linkages. McGraw-Hill, New York
89. Morrey BF, Chao EY (1976) Passive motion of the elbow joint. J Bone Jt Surg Am 58:501–508
90. Jeannerod M (1995) Mental imagery in the motor context. Neuropsychologia 33(I1):1419–1432. doi:10.1016/0028-3932(95)00073-C
91. Collet C, Guillot A (2010) Autonomic nervous system activities during imagined movements. In: Guillot A, Collet C (eds) The neurophysiological foundations of mental and motor imagery. Oxford University Press, New York, pp 95–108
92. Contreras-Vidal JL, Stelmach GE (1995) A neural model of basal ganglia-thalamocortieal relations in normal and parkinsonian movement. Biol Cybern 73:467–476
93. Frak V, Cohen H, Pourcher E (2004) A dissociation between real and simulated movements in Parkinson's disease. Neuroreport 15:1489–1492
94. Hétu S, Grégoire M, Saimpont A, Coll MP, Eugène F, Michon PE, Jackson PL (2013) The neural network of motor imagery: an ALE meta-analysis. Neurosci Biobehav Rev 37:930–949
95. Lotze M, Halsband U (2006) Motor imagery. J Physiol Paris 99:386–395
96. Sauvage C, Jissendi P, Seignan S, Manto M, Habas C (2013) Brain areas involved in the control of speed during a motor sequence of the foot: real movement versus mental imagery. J Neuroradiol 40(4):267–80. doi:10.1016/j.neurad.2012.10.001
97. Lau HC, Rogers RD, Haggard P, Passingham RE (2004) Attention to Intention. Science 20:303(5661): 1208–1210

98. Herrero MT, Barcia C, Navarro JM (2002) Functional anatomy of thalamus and basal ganglia. Childs Nerv Syst 18:386–404. doi:10.1007/s00381-002-0604-1
99. Jeannerod M (2006) Motor cognition. Oxford University Press, New York
100. Lotze M, Montoya P, Erb M, Hulsmann E, Flor H, Klose U, Birbaumer N, Grodd W (1999) Activation of cortical and cerebellar motor areas during executed and imagined hand movements: an fMRI study. J Cogn Neurosci 11:491–501
101. Aron AR, Durston S, Eagle DM, Logan GD, Stinear CM, Stuphorn V (2007) Converging evidence for a fronto-basal-ganglia network for inhibitory control of action and cognition. J Neurosci 27:11860–11864
102. Bonnet M, Decety J, Jeannerod M, Requin J (1997) Mental simulation of an action modulates the excitability of spinal reflex pathways in man. Brain Res Cogn Brain Res 5:221–228
103. Bradberry TJ, Gentili RJ, Contreras-Vidal JL (2010) Reconstructing three-dimensional hand movements from noninvasive electroencephalographic signals. J Neurosci 30(9):3432–3437. doi:10.1523/JNEUROSCI.6107-09.2010
104. Visalberghi E, Limongelli L (1996) Action and understanding: tool use revisited through the mind of capuchin monkeys. In: Russon A, Bard K, Parker S (eds) Reaching into thought. The minds of the great apes. Cambridge University Press, Cambridge, pp 57–79
105. Gentili RJ, Oh H, Molina J, Reggia JA, Contreras-Vidal JL (2012) Cortex inspired model for inverse kinematics computation for a humanoid robotic finger. In: Proceedings of annual international conference of the IEEE Engineering in Medicine and Biology Society, pp 3052–3055. doi:10.1109/EMBC.2012.6346608
106. Pedreño-Molina JL, Molina-Vilaplana J, López-Coronado J, Gorce P (2005) A modular neural network linking Hyper RBF and AVITE models for reaching moving objects. Robotica 23(05):625. doi:10.1017/S0263574704001055
107. Nishimoto R, Tani J (2009) Development of hierarchical structures for actions and motor imagery: a constructivist view from synthetic neuro-robotics study. Psychol Res 73:545–558. doi:10.1007/s00426-009-0236-0
108. deJong R, Coles MG, Logan GD, Gratton G (1990) In search of the point of no return: the control of response processes. J Exp Psychol Hum Percept Perform 16:164–182
109. Sylvester JC, Reggia JA, Weems SA, Bunting MF (2013) Controlling working memory with learned instructions. Neural Netw 41:23–38. doi:10.1016/j.neunet.2013.01.010
110. Jeannerod M (1994) The representing brain: neural correlates of motor intention and imagery. Behav Brain Sci 17:187–202
111. Guillot A, Lebon F, Rouffet D, Champely S, Doyon J, Collet C (2007) Muscular responses during motor imagery as a function of muscle contraction types. Int J Psychophysiol 66:18–27
112. Slade JM, Landers DM, Martin PE (2002) Muscular activity during real and imagined movements: a test of inflow explanations. J Sport Exerc Psychol 24:151–167
113. Lebon F, Rouffet D, Collet C, Guillot A (2008) Modulation of EMG power spectrum frequency during motor imagery. Neurosci Lett 435:181–185
114. Oztop E, Bradley NS, Arbib MA (2004) Infant grasp learning: a computational model. Exp Brain Res 158:480–503. doi:10.1007/s00221-004-1914-1
115. Oztop E, Kawato M, Arbib MA (2013) Mirror neurons: functions, mechanisms and models. Neurosci Lett 540:43–55. doi:10.1016/j.neulet.2012.10.005
116. Schweighofer N, Arbib MA, Kawato M (1998) Role of the cerebellum in reaching movements in humans. I. Distributed inverse dynamics control. Eur J Neurosci 10(1):86–94

Rodolphe J. Gentili is currently an Assistant Professor in the Department of Kinesiology and a faculty member in the Neuroscience and Cognitive Science Program as well as the Maryland Robotics Center at the University of Maryland-College Park (USA). His research examines the underlying cognitive-motor processes of adaptive human performance by employing a combination of experimental and computational approaches. This allows for an integrative perspective on human motor behavior and for the development of neuromimetic control systems that are able to adaptively control humanoid robotic upper limbs as well as interact with humans through human–machine interfaces.

Hyuk Oh is a Ph.D. candidate in the Neuroscience and Cognitive Science Program at the University of Maryland-College Park (USA). He received his B.Sc. in Computer Science from the Seoul National University (South Korea) in 1999 and then his M.S. in Computer Science from the University of Southern California (USA) in 2006. His research interests include computational models of the human sensorimotor system with emphasis on imitation learning, and neural dynamics in cognitive-motor processes using various non-invasive brain biomarkers and physiological sensors.

Di-Wei Huang is a Ph.D. candidate in Department of Computer Science, University of Maryland, College Park, United States. He received an MS degree in Computer Science and Information Engineering (CSIE) at National Taiwan University in 2006, and a B.S. degree in CSIE at National Chiao-Tung University, Taiwan, in 2004. His current research interests include neural computation and cognitive robotics, with specific emphasis on neural dynamics and neurocognitive architectures.

Garrett E. Katz is a research assistant and doctoral student at the University of Maryland, College Park, focusing on bio-inspired artificial intelligence. Garrett received a B.A. in Philosophy from Cornell University and an M.A. in Mathematics from City College of New York. Previously Garrett worked as a research technician at City College, focusing on computerized tomography of biological viruses.

Ross H. Miller is received his Ph.D. in kinesiology in 2011 from the University of Massachusetts. He is currently an Assistant Professor in the Department of Kinesiology at the University of Maryland, College Park. His research focuses on using musculoskeletal modeling to understand the mechanics and control of human movement in health and pathology.

James A. Reggia is a Professor of Computer Science at the University of Maryland at College Park, with joint appointments in the Institute for Advanced Computer Studies and in the Department of Neurology of the School of Medicine. His research interests are in the areas of neural computation, artificial life, evolutionary computation, and artificial intelligence, and he has authored numerous research papers in these areas.